Dynamic spatial coding in parietal cortex mediates hand movement planning towards touch

Janina Klautke [1,#], Celia Foster [2,3], W. Pieter Medendorp [4], Tobias Heed [2,3,5,6*]

[1] Biological Psychology and Neuropsychology, University of Hamburg, Hamburg, Germany

[2] Biopsychology & Cognitive Neuroscience, Bielefeld University, Bielefeld, Germany

[3] Center of Excellence in Cognitive Interaction Technology (CITEC), Bielefeld University, Bielefeld, Germany

[4] Radboud University, Donders Institute for Brain, Cognition and Behaviour. Nijmegen, The Netherlands

[5] Cognitive Psychology, Department of Psychology, University of Salzburg, Salzburg, Austria

[6] Centre for Cognitive Neuroscience, University of Salzburg, Salzburg, Austria

[#] Janina Klautke has previously published under the last name Brandes.

[*] Correspondence and requests for materials should be addressed to T.H. (email: tobias.heed@plus.ac.at)

Abstract

Movements towards touch on the body require integrating tactile location and body posture information. Tactile processing and movement planning both rely on posterior parietal cortex (PPC) but their interplay is not understood. Here, human participants pointed towards or away from memorized tactile stimuli on their feet, dissociating sensory and motor locations. Participants crossed or uncrossed their feet to dissociate stimulus location relative to anatomy versus in external space. Multi-voxel pattern analysis of concurrently recorded fMRI signals revealed that tactile location was coded anatomically in anterior PPC but spatially in posterior PPC during sensory processing. After movement instructions were specified, PPC exclusively represented the movement goal in space, in regions closely matching those that mediate visuomotor planning and with regional overlap for sensory, rule-related, and movement coding. Thus, PPC flexibly updates its spatial codes to accommodate rule-based transformation of arbitrary sensory input to generate movement to environment and own body alike.

Keywords

Touch, sensorimotor transformation, movement planning, tactile remapping, anti-task

Introduction

We frequently make reaching movements to tactile stimuli, for example to scratch an itch, move a hair away from our face, or to brush off an insect that crawls along our arm. We perform these movements with ease even though the brain must make complex computations to successfully complete them. Tactile stimulation excites receptors in the skin, and thus tactile location is initially coded relative to the skin's layout as is evident, for instance, in the homuncular organization of primary somatosensory cortex (S1)[1,2]. Yet, the skin is but a 2D sheet wrapped around our 3D body which, in addition, constantly changes its layout when the body parts move. Therefore, planning movement towards a touch presumably requires transformation of tactile information from skin-based, anatomical coding into a 3D spatial code – often referred to as remapping from a somatotopic or anatomical into an external(-spatial) reference frame[3]–, based on the integration of body knowledge and posture information[3,4]. The external-spatial reference frame could code stimuli relative to different body parts, for instance the line of gaze, the position of the head or torso, or in a reference frame that integrates several such reference points[5].

In comparison to movement planning towards visual targets, tactually guided movement adds considerable complexity to body coordination. During reaches towards a visual target, body-related processing is primarily concerned with coordinating the reaching effector for the movement; in contrast reaching towards a tactile stimulus additionally requires processing body information about the movement target as well as relating the tactile target and moving effector, which both belong to the same body. One puzzle about this double role of the body being the movement target and the moving entity is that both touch and movement processing recruit the posterior parietal cortex (PPC). To date, there is little knowledge about how sensory and motor roles of PPC are integrated.

The somatotopic organization evident in S1 extends into the anterior regions of PPC in both macaques[6] and humans[7,8]. In contrast, magneto- and electroencephalographic brain signals over parietal cortex are modulated by both the somatotopic and external-spatial location of tactile stimuli[9–11], yet the spatial resolution of these methods limits conclusions about which brain regions use the respective spatial codes to large areas. Generally speaking, somatotopic coding appears to occur more anteriorly than external coding. Transcranial magnetic stimulation (TMS) has also provided evidence that PPC encodes tactile location in an external-spatial reference frame[12–14]. However, though it appears established that PPC uses both somatotopic and external-spatial coding for touch, it has remained elusive which parietal regions employ which code and how transformations between them occur.

Research on sensorimotor transformation has often focused on visuomotor paradigms; these studies are, therefore, an obvious starting point for establishing the principles that underly tactile-motor processing. Studies on visuomotor transformation have established that posterior PPC regions encode visual targets for hand reaches in a gaze-centered reference frame[15–22] while anterior PPC regions encode them in a hand-centered reference frame[23–30]. In contrast in the macaque ventral intraparietal cortex, visual receptive fields are linked to tactile receptive fields, such that the visual space relevant to a given neuron changes when the monkey moves the body part to which the tactile receptive field is linked[31–33]. However, the reference frames employed by parietal regions are often not fixed but can vary depending

on the available information or task requirements[16,34,35]. Thus, spatial coding in this cortical region is dynamic, and such dynamics have been demonstrated not only between different contexts but also during the progression of single trials, marking PPC as a key region of sensorimotor transformation.

We have so far addressed direct spatial transformations, which transform the location of a sensory stimulus into a code that guides the motor system to that very location. Thus, such transformations mediate directly between sensory and motor reference frames. However, parietal cortex is also involved in deriving movement plans from arbitrary, abstract sensory cues[36–38]. In such paradigms, the sensory stimulus and movement goal are not identical in their location. For instance, movements depend on rules when a movement must not be directed directly to a visual cue but, instead, a different movement goal must be inferred based on the cue's location. A typical paradigm is the so-called anti-movement task, in which participants must plan a response to either the location of a cue, or a location opposite from it[39–43]. In the latter case, the movement goal location is in a different spatial location than the sensory cue, which allows brain responses related to sensory processing and movement planning to be distinguished. In experiments that employed this paradigm, PPC neurons first encoded the location of a visual cue, but later switched to encoding the location of the movement goal[40,44]. Human PPC also exhibits such dynamic coding, with responses to visual cues before the movement goal is specified, but representing movement plans once the reach goal has been specified[41,45–48]. In sum, neuronal responses in PPC can reflect the evolution of a spatially specific motor plan based on sensory information and task instruction. Accordingly, parietal computations go beyond mere transformations of spatial location between different reference frames and are flexibly adapted to the current task or behavioral goal.

Even if it seems without question that PPC dynamically mediates between different spatial codes, it is not clear whether and how the principles uncovered in visuomotor research generalize to situations in which movements target the own body. Anterior PPC is involved in coding posture and body configuration in the context of reaching tasks without vision[49–51], and a frontoparietal network, including a wide area of PPC, encodes proprioceptive reach targets in a body-centred code[16,35]. Notably, however, paradigms that investigate movement planning to proprioceptive targets usually name the target body part (e.g., "move to the tip of the left index finger"). Therefore, this type of task does not involve the transformation of tactile information from skin into space and tests only one aspect of somatosensation, namely proprioception but not touch. Studies that have addressed touch have demonstrated that PPC mediates sensorimotor transformation of tactile targets on the hands[9,52,53]. However, the respective studies did not dissociate sensory and motor spatial information and so it remains unclear whether the observed responses were related to maintained sensory processing or to movement planning.

Viewed together, there are three dissociable spatial codes in reaches to tactually stimulated locations on one's body: (1) somatotopic and (2) external-spatial locations of the tactile stimulus, and (3) a motor goal location. Moreover, the latter may have to be derived via a task rule. In the present study, we mapped the emergence of information related to these three spatial codes, as well as to the task rule, during a tactile-motor task. We recorded fMRI while human participants planned and executed hand pointing movements to tactile stimuli presented on their feet, which were positioned either uncrossed or crossed. A given tactile

stimulus is located on the opposite side of space with uncrossed vs. crossed feet; therefore, this manipulation allowed us to dissociate anatomical and external-spatial coding of tactile targets. Moreover, we employed an anti-pointing task rule, which allowed us to differentiate tactile sensory processing from motor-related, sensorimotor transformation. Thus, the combination of foot posture and pro/anti-pointing allowed us to fully dissociate anatomical and external-spatial coding of tactile targets, as well as movement coding to these tactually-defined sensory targets.

Results

Experimental setup and analysis rationale. Fig. 1 illustrates the trial design. Each trial was separated into four intervals, beginning with a fixation interval. Participants were then presented with a tactile stimulus on their left or right foot, followed by a delay, forming the touch localization interval (duration: 1-4 TR = 1880-7520 ms). There were two stimulus locations on each foot, located medially and laterally on the back of each foot, approximately two centimeters below the heads of the metatarsal bones. These two locations encouraged participants to plan precise pointing movements rather than just making a stereotypical response to one side or the other. Participants learned the present trial's task rule via a visual cue only after the touch localization interval: either a right-hand pointing movement toward the remembered stimulus location (pro-pointing) or an anti-pointing movement to the homologous location on the other foot. This instruction was followed by another delay, forming the movement planning interval (duration: 1-4 TR = 1880-7520 ms). A cue at the end of this interval prompted movement execution. Because the required movement was specified only after the touch localization interval, the final required movement was unknown during this time interval, and therefore we expect that activation in the touch localization interval is related exclusively to stimulus processing. In contrast, activation in the movement planning interval may be related not only to movement planning, but may also retain spatial

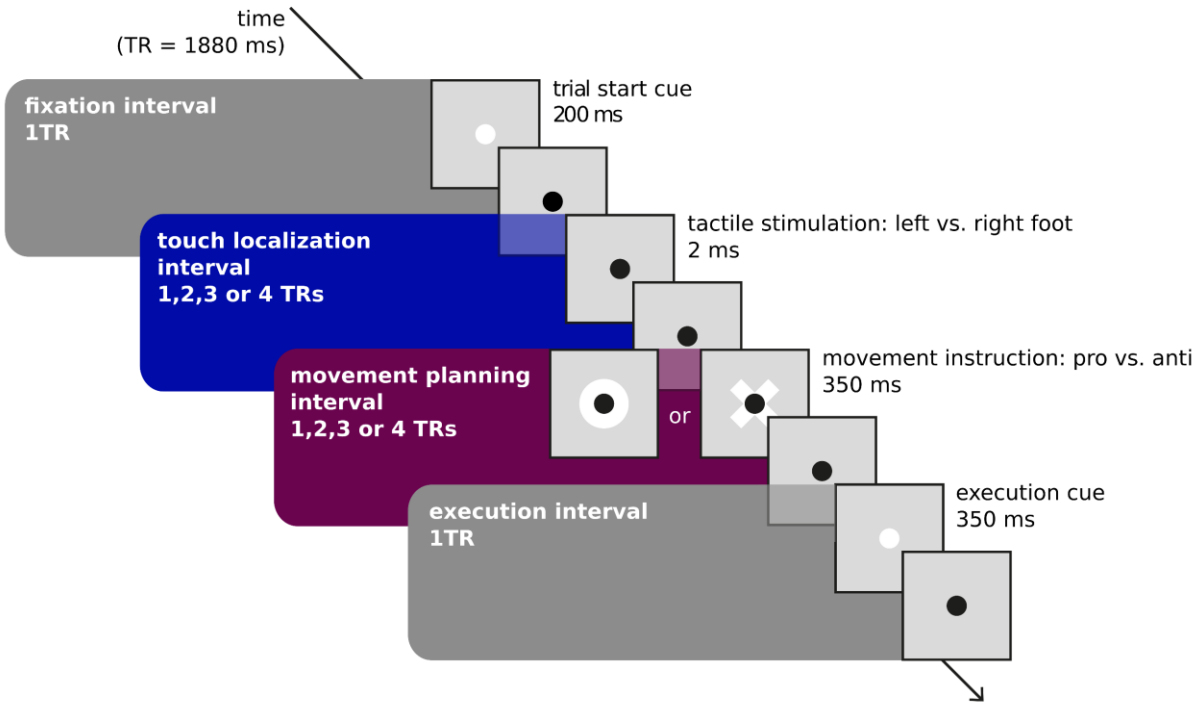

Fig. 1 Task design. A central black fixation dot was present at all times. This fixation dot briefly turned white to indicate the beginning of a trial and was followed by a 1TR (1880 ms) fixed time interval. Next, a tactile stimulus was presented to the left or right foot, followed by delay of variable duration (1-4 TR = 1880-7520 ms). A visual cue then instructed the required movement: a circle instructed pro-pointing of the right hand towards the tactile stimulus; a cross instructed anti-pointing to the homologous location on the other foot. This movement instruction cue was followed by a delay of variable duration (1-4 TR = 1880-7520 ms). Lastly, the fixation dot turned white to prompt movement execution, which was followed by a fixed 1 TR (1880 ms) movement execution interval.

information about the stimulus. Participants were highly accurate in pointing movements for trials in which hand movement tracking could be assessed (66% of trials), with a mean accuracy of 92% in making movements to the correct location. A 2 (left vs right tactile stimulation) x 2 (uncrossed vs crossed posture) x 2 (pro vs anti task) within-subjects repeated measures ANOVA showed no main effect of tactile stimulation location ($F_{1,15} = 2.75$, $p = .12$, $\eta_p^2 = 0.15$), posture ($F_{1,15} = 0.69$, $p = .42$, $\eta_p^2 = 0.04$) or task rule ($F_{1,15} = 0.05$, $p = .83$, $\eta_p^2 = 0.00$) on task accuracy, or any interaction between the three factors. Thus, participants were similarly accurate across conditions.

Multi-voxel pattern analysis (MVPA) was performed to assess whether a classifier trained to dissociate fMRI voxel activation patterns observed during one trial class (e.g., trials with a tactile stimulus at the left foot) vs. another trial class (e.g., trials with a tactile stimulus at the right foot) can predict the correct class label of new activation patterns that were not used during training. We used a searchlight procedure[54] that decodes patterns of voxels contained in a sphere with a 4-voxel radius around a center voxel. Each of the brain's voxels serves once

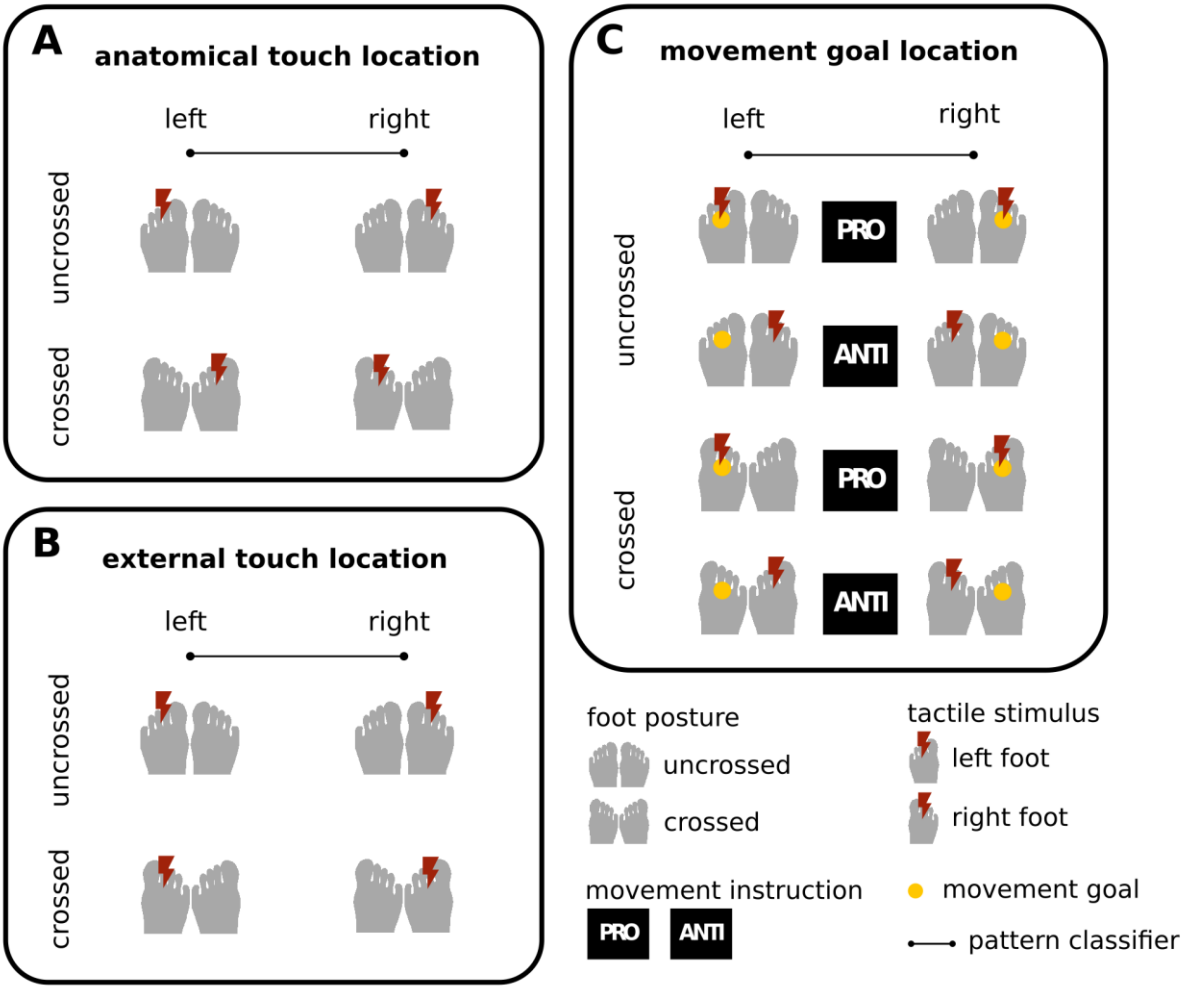

Fig. 2 Overview of MVPA decoding analyses. **A** Conditions for decoding anatomical touch location (left vs. right foot). **B** Conditions for decoding external touch location, i.e., spatial side of touch. Note, that foot crossing dissociates anatomical from external location. **C** Conditions for decoding the location of the movement goal. The combination of foot posture, stimulation side, and pro/anti-pointing dissociates sensory and movement coding. A more detailed illustration of the MVPA decoding analyses is shown in Fig. S1.

as the center voxel, so that the procedure generates a brain-wide map of decoding accuracy. When decoding performance is significantly above chance, the sphere around the respective center voxel contains differences in the patterns of neural responses that can distinguish between the two tested classes. Accordingly, we interpret significant decoding as indicating that the respective region encodes information related to the tested task characteristic.

Classification analyses devised for the present study are summarized in Fig. 2 and specified in detail in Fig. S1. We additionally performed univariate analyses to test whether any regions showed overall differences in activity between our main conditions of interest (see Supplemental Information).

Anatomical and external spatial coding are present during tactile-sensory processing. We first tested whether information about anatomical and external touch location was present in activity patterns during the touch localization interval, when sensory information was available but the movement goal was not yet specified. Anatomical touch location identifies which of the two feet, right or left, received stimulation, independent of where the respective foot was currently placed. The conditions contrasted in our MVPA decoding are illustrated in Fig. 2A and Fig. S1A (left side, within-interval classifier 1).

Anatomical information was present in multiple parietal regions (Fig. 3A and Table 1): the medial bank of primary somatosensory cortex (S1), bilaterally; the lateral right inferior parietal lobule (IPL), bordering secondary somatosensory cortex (S2) and spreading to lateral S1 and primary motor cortex (M1); and the left anterior SPL. Decoding was also successful outside parietal cortex, in the right PMd and the left insula, spreading into the superior temporal gyrus. The group mean, above-chance decoding accuracy ranged from 53.8-55.0%, with participant-level confidence intervals ranging from 0.3% to 2.0% (Fig. 3B). These classification values are in a range that is typical for MVPA decoding[46,55–59].

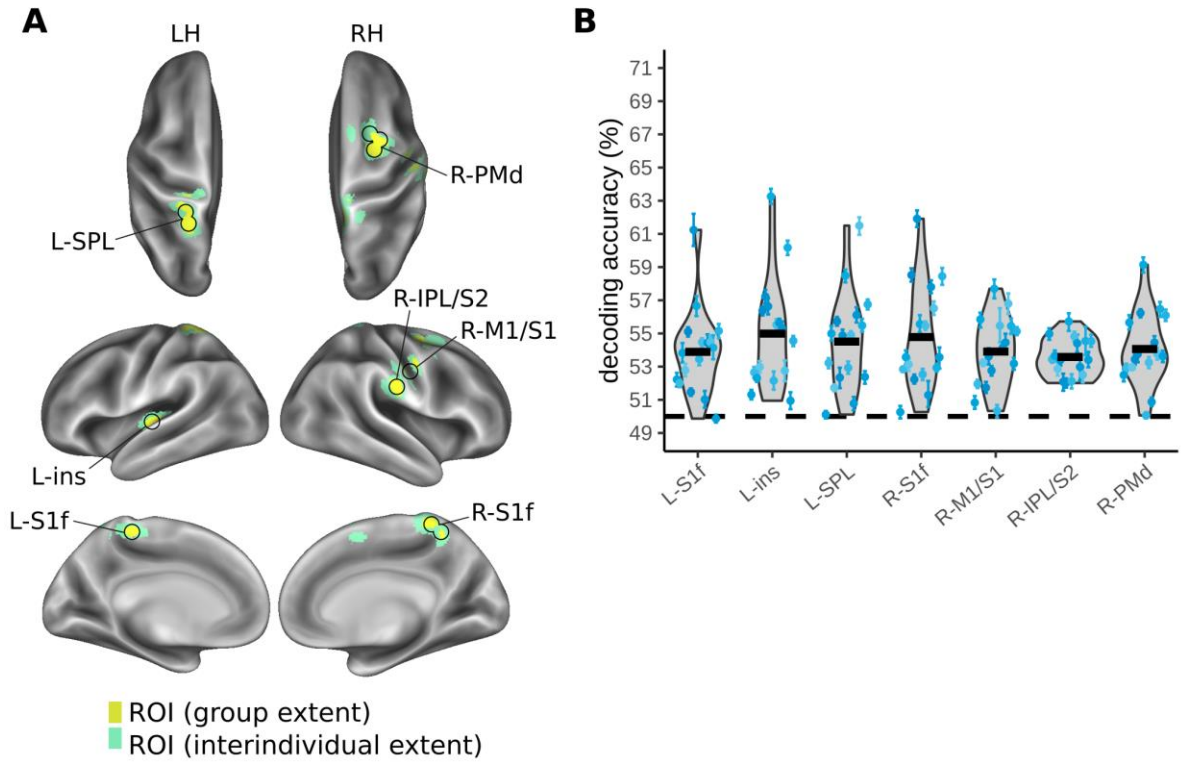

Fig. 3 MVPA results for decoding anatomical touch location (right vs. left foot) during the touch localization interval. An overview of the conditions organized for decoding anatomical touch location is shown in Fig. 2A. **A** Regions of interest (ROI) identified based on a group-level statistical map. The yellow color indicates the extent of the group-level activation, corrected for multiple comparisons using a cluster-based permutation test (FWE, p <.05). The green color indicates the spread of the ROI based on region identification for each individual (see Methods) **B** Violin plots illustrate variability of individual decoding accuracy across participants for each ROI (grey shading, black outlines). The dashed black line indicates chance decoding (50%). The thick black horizontal bars indicate the participant group's grand mean decoding accuracy. The blue scatter points indicate individual means for each participant and the error bars around these individual means represent individual bootstrapped 95% confidence intervals of decoding accuracy. Axis limits correspond with those of Figs. 4, 5, 6 to facilitate comparison across analyses. LH, left hemisphere; RH, right hemisphere. L-S1f, foot area of left primary somatosensory cortex; L-ins, left insula; L-SPL, left superior parietal lobule; R-S1f, foot area of right primary somatosensory area; R-M1/S1, right primary motor cortex/ primary somatosensory cortex; R-IPL/S2, right inferior parietal lobule/ secondary somatosensory cortex, R-PMd, right dorsal premotor cortex.

External touch location identifies on which side of external space, the right or left side, a stimulus occurred, independent of which foot the stimulus was applied to. Foot crossing dissociates external from anatomical location as, for example, both the uncrossed left foot and the crossed right foot are located on the left side of space. The conditions contrasted in MVPA decoding are illustrated in Fig. 2B and Fig. S1B (left side, within-interval classifier 2). External touch location information was present in a single, right-lateralized cluster confined to the medial IPS (Fig. 4A and Table 1). The group mean, above-chance decoding accuracy was 54.4% with participant-level confidence intervals ranging from 0.4-1.4% (Fig 4B).

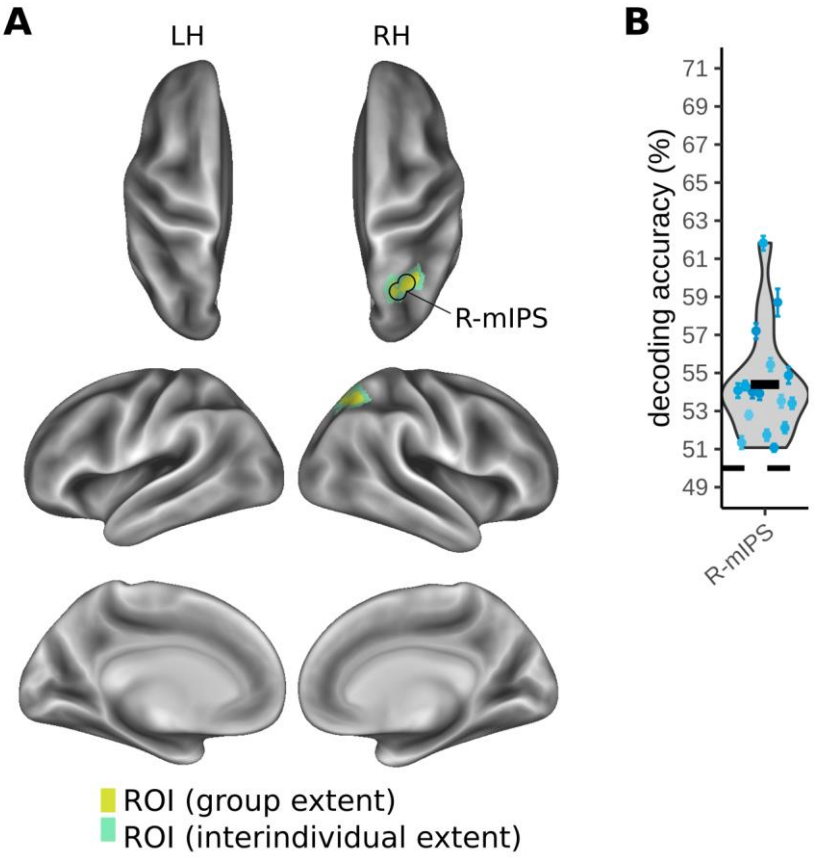

Fig. 4 MVPA results for decoding external touch location (right vs. left side of space) during the touch localization interval. An overview of the conditions organized for decoding external touch location is shown in Fig. 2B. **A** Right medial IPS (R-mIPS) ROI identified based on a group-level statistical map. The yellow color indicates the extent of group-level activation, corrected for multiple comparisons using a cluster-based permutation test (FWE, p <.05). The green color indicates the spread of the ROI based on region identification for each individual (see Methods) **B** Variability of individual decoding accuracy across participants in R-mIPS. Conventions as in Fig. 3.

Tactile-sensory spatial codes are maintained only as long as necessary. Previous research has suggested that neurons change their spatial tuning during sensorimotor processing[44,45]. Therefore, we next tested whether anatomical and external spatial information about the tactile stimulus remained stable across touch localization and movement planning intervals. We used the classifiers trained in the touch localization interval to classify voxel patterns in the movement planning interval[60]. Successful cross-interval classification would suggest that tactile stimulus coding was maintained across both touch localization and movement planning intervals. In contrast, a failure of cross-interval classification would imply a change in the representational format, as evident in voxel-wise brain activity, across the trial phases.

The conditions we pooled in these analyses are illustrated in Fig. S1 (anatomical location information: Fig. S1A, middle, cross-interval classifier 3; external location information: Fig. S1B, middle, cross-interval classifier 4). These classifiers did not identify any regions in which decoding of touch location across trial phases was above chance. We additionally tested cross-classification of sensory coding separately for pro- and anti-pointing conditions, as it would be possible that a default motor plan could be made in the tactile localization interval towards the target, that would then be remapped for anti-pointing trials upon receiving the task cue.

We did not identify any regions that allowed decoding touch location across trial phases for either pro-pointing or anti-pointing trials, suggesting that participants did not prepare a default motor plan to the tactile stimulus during the tactile localization interval. Altogether, the results of these analyses suggest that spatial coding differs between the two trial phases for all regions.

However, even if coding patterns changed from one trial phase to the next, it would still be possible that stimulus-related, anatomical information or external, spatial information is encoded via a different neuronal firing pattern or in different neurons and, thus, expressed in different voxel patterns. To test whether tactile-sensory spatial information is retained during the movement planning interval with an altered coding strategy, we trained classifiers to differentiate anatomical and external target locations with data from the movement planning interval and tested them on their ability to predict the target locations of test data from the same interval (anatomical: Fig. S1A, right side, within-interval classifier 5; external: Fig. S1B, right side, within-interval classifier 6). Neither classifier identified significant decoding in any region of the cortex. Altogether these classification results indicate that once participants could prepare the movement, sensory information was no longer retained, or was retained at a level too low to be detected by our classification analysis – and, thus, at a level lower than that during the touch localization interval.

In sum, PPC appears to maintain tactile-sensory spatial information only as long as necessary and discard it, or massively reduce its representation, once it can transform sensory information into a motor response. Notably, the two spatial codes were prevalent in distinct PPC regions, without any regional overlap.

Tactile-motor planning recruits a similar network of fronto-parietal regions as visuo-motor planning. Having established that sensory spatial information is decodable only in the touch localization interval, we next tested which brain regions contain information about the tactually defined spatial location of the movement target during the movement planning interval. The movement goal location identified the location in external space (right or left side) to which a hand pointing movement would be directed; we pooled across all possible stimulus locations on a given foot and decoded only left and right side of space, rather than the exact spatial location. Fig. 2C illustrates how the combination of foot posture, stimulus location, and pro vs anti-movement dissociates the location of the movement goal from both anatomical and external stimulus locations in our classification analysis. For example, a pro-pointing movement to the left uncrossed foot, an anti-pointing movement to the left crossed foot, and a pro pointing movement to the right crossed foot all require an identical, left-directed pointing movement but do not consistently share anatomical or external stimulus locations, nor their task rule.

MVPA classification of movement goal location during the movement planning interval (right vs. left movement target, Fig. S1C, within-interval classifier 7) identified widespread above-chance classification in parietal areas, including bilateral S1, M1, and SPL, as well as bilateral frontal areas PMd and SMA (Fig. 5 and Table 1). Above-chance classification was identified in more extensive regions in the left hemisphere, the hemisphere contralateral to the effector that executed the pointing movement. Here, above-chance classification was also evident in parietal cortex along the IPS and in the parietal occipital sulcus (POS), and in frontal cortex in the pre-SMA. In the right hemisphere, a small additional cluster was identified in the

occipitotemporal cortex. The group mean above-chance decoding accuracy ranged from 54.1-58.4% in the left hemisphere and from 53.8-58.0% in the right hemisphere, with participant-level confidence intervals ranging from 0.3-2.4% and from 0.3-2.6% respectively (Figure 5B). In a univariate analysis that identified regions more active for right than left pointing targets, we identified clusters in the bilateral SMA and the left lateral and medial anterior SPL, M1 and the PMd that showed stronger activation for planning pointing movements to right targets as compared to left targets (Fig. S3).

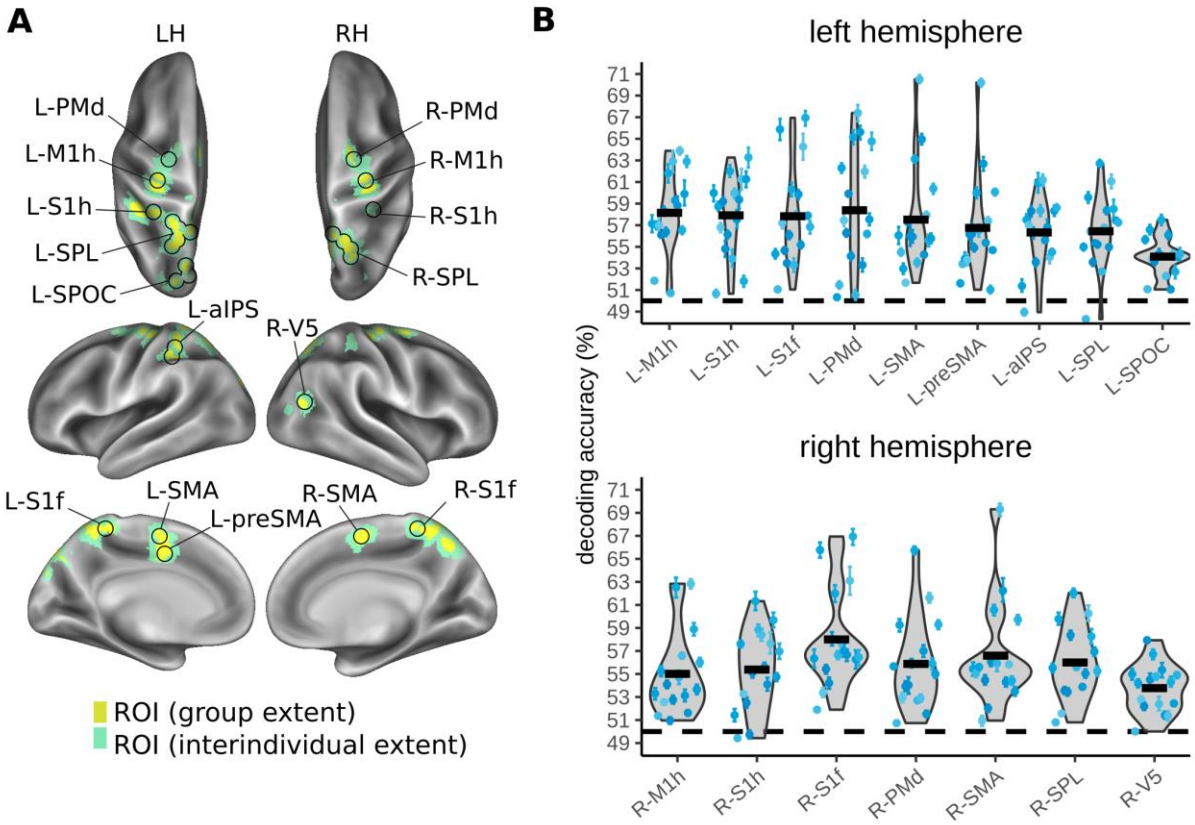

Fig. 5 MVPA results for decoding movement goal location (pointing movement to the foot on the right or left side of space) during the movement planning interval. An overview of the conditions organized for decoding movement goal location is shown in Fig. 2C. **A** ROIs identified based on a group-level statistical map. **B** Variability of individual decoding accuracy across participants in the different ROIs. Conventions as in previous figures. L-M1h, hand area of left primary motor cortex; L-S1h, hand area of left primary somatosensory cortex; L-PMd, left dorsal premotor cortex; L-SMA, left supplementary motor area; L-preSMA, left pre-supplementary motor area; L-aIPS, left anterior intraparietal sulcus; LSPL, left superior parietal lobule; L-SPOC, left superior parieto-occipital cortex; R-M1h, hand area of right primary motor cortex; R-S1h, hand area of right primary somatosensory cortex; R-PMd, right dorsal premotor cortex; R-SMA, right supplementary motor area; R-SPL, right superior parietal lobule; R-V5, right middle temporal visual area.

The vast, bilateral responses related to the goal location during the movement planning interval differed markedly from the more regionally confined responses related to sensory spatial information. This is consistent with previous reports of stronger PPC activation during motor planning than sensory processing in sensorimotor delay paradigms such as the current one[61,62], underlining the prominent involvement of PPC in motor planning and control[40,63].

PPC encodes the current task rule. Our task required participants to interpret the task rule, i.e., pro- vs. anti-pointing, to derive the required movement from the tactile location. Participants showed similar mean task accuracy for both pro- and anti-pointing (both 92% correct). In the macaque PPC, the task rule is encoded independent of specific sensory cues[64], and it modulates neuronal firing in the areas that encode the movement goal[40]. Human fMRI studies did not find differences in univariate activation between preparation of pro- and anti-pointing movements[41,45], nor were they able to decode pro- vs. anti-pointing from regions of interest in the SPL, aIPS or PMd[46]. We tested whether we could decode the task rule in our tactile-motor task. Fig. 6 illustrates the performance of a classifier trained to dissociate pro- and anti-pointing movements during the movement planning interval (Figure S2, within-interval classifier 8). Average ROI coordinates across participants are displayed in Table 1. Task rule could be decoded above chance-level bilaterally in the SPL and in the left superior parieto-occipital cortex (SPOC). The mean above-chance decoding accuracy of the task rule per ROI ranged from 53.8% to 54.1% with participant-level confidence intervals covering ranges from 0.3% to 1.3% (Fig. 6B).

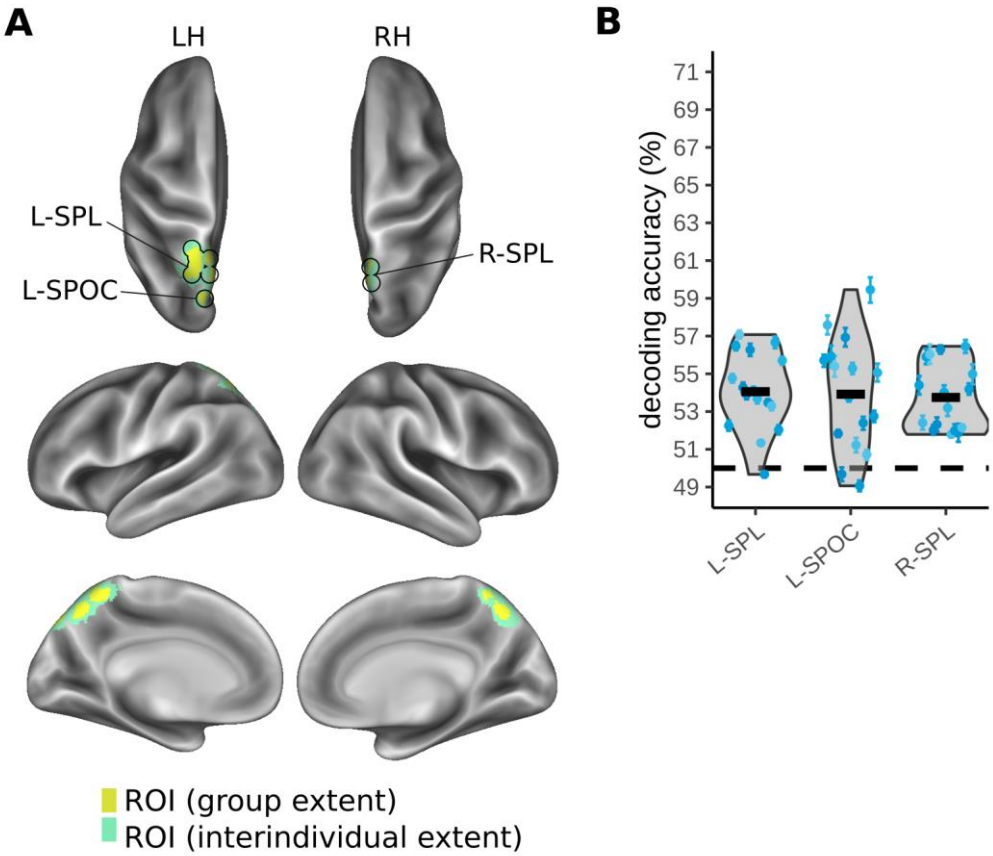

Fig. 6 MVPA results for decoding task rule (pro- vs. anti-pointing movement) during the movement planning interval. **A** ROIs identified based on a group-level statistical map. **B** Variability of individual decoding accuracy across participants in the different ROIs. Conventions as in previous figures. L-SPL, left superior parietal lobule; L-SPOC, left superior parieto-occipital cortex; R-SPL, right superior parietal lobule.

From touch localization to sensorimotor planning: functional overlap. Our results demonstrate that PPC contains anatomically and externally coded tactile information during the touch localization interval and information about the motor goal and task rule during the movement planning interval. We next explored whether there was overlap between the regions that encoded sensory and motor-related spatial information in the two intervals. Such an overlap would provide evidence for a dynamic change in spatial coding within areas across the duration of a trial, likely implying that the same regions are involved in the underlying transformation between the different spatial codes over the course of sensorimotor processing.

Figure 7 displays the overlap between clusters in which our classifiers identified sensory and motor-related spatial coding. There is considerable overlap between these spatial codes across trial intervals. 34% of the voxels that encoded the anatomical stimulus location during the stimulus localization interval overlapped with voxels identified as coding movement goal location in the movement planning interval. These overlapping voxels were located in S1 bilaterally, as well as the left SPL and the right PMd (Fig. 7A; overlap: 221 voxels = 5967 mm^3). 61% of the voxels that encoded external stimulus location during the stimulus localization interval overlapped with voxels that coded movement goal location. These voxels were located in the right mIPS (Fig. 7B; overlap: 74 voxels = 1998 mm^3). Thus, a considerable proportion of voxels participated in coding spatial stimulus information in one reference frame in the first trial interval, and spatial movement goal information in a different reference frame in the second trial interval.

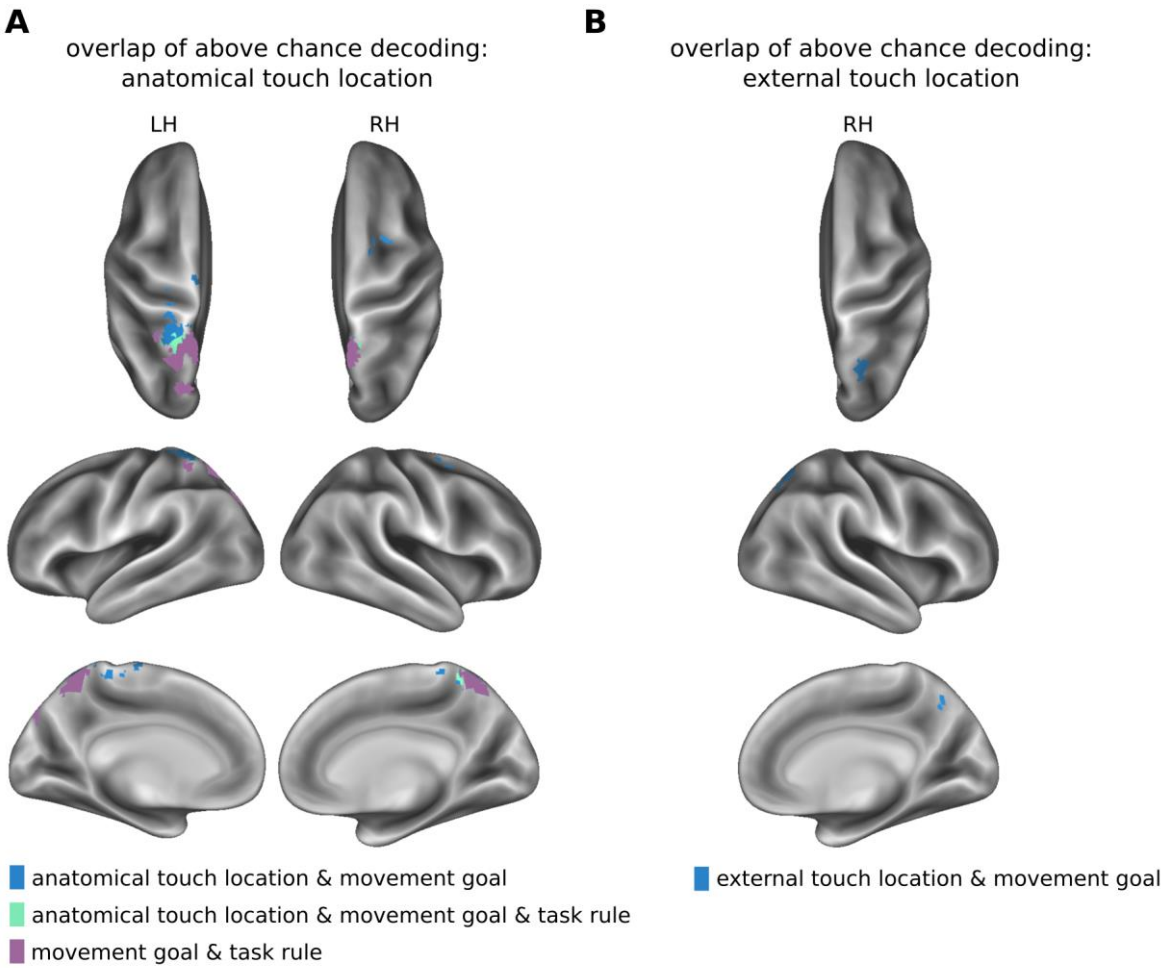

Fig. 7 Overlap of clusters encoding information about anatomical or external touch location, movement goal location, and task rule. **A** Overlap with regions that encode anatomical touch location. **B** Overlap with regions that encode external touch location. LH, left hemisphere; RH, right hemisphere.

Furthermore, 90.4% of the cluster representing the task rule overlapped with the cluster representing movement goal locations bilaterally in the SPL and in the left POS (overlap of 422 voxels, volume: 11,394 mm^3; Figure 7A). In the left SPL, located between voxels common to anatomical and movement goal location and voxels common to goal location and task rule, was a voxel overlap of all three types of information (overlap of 34 voxels, volume: 1161 mm^3; Figure 7A). This finding implies that the prevalent information coded in these regions, as decodable with MVPA, varies over the course of the trial and, thus, that the neural function of these regions changes over time: PPC regions that coded tactile location before a movement plan could represent the movement goal once the task rule had been specified. Moreover, areas that carried information about the task rule were almost completely enclosed within the cluster that coded movement goal location, suggesting that this bilateral PPC region performs a sensorimotor transformation based on stimulus location and task rule, to turn this information into a movement goal.

317 ## Discussion

318 We investigated the reference frames involved in tactile-motor transformation during
319 pointing to tactually indicated locations on the feet. We dissociated anatomical and external-
320 spatial coding of tactile stimuli by manipulating whether participants' feet were uncrossed or
321 crossed, and further dissociated between sensory and motor-related responses using a
322 delayed anti-task paradigm. We report three key findings. First, PPC exhibited concurrent
323 anatomical and external-spatial coding of tactile stimulus location in different PPC regions
324 during the touch localization interval. Anterior regions including primary somatosensory
325 cortex and SPL encoded stimuli in an anatomical reference frame, whereas medial IPS, located
326 in the posterior PPC, encoded stimuli in an external spatial reference frame. Second, spatial
327 coding was dynamic, showing responses related to stimulus location prior to presentation of
328 the task rule, and then responses encoding the motor goal location following presentation of
329 the task rule. There was also overlap between regions encoding first sensory and later motor
330 information, and one region in SPL coded the original anatomical stimulus location, the task
331 rule, and the resulting movement goal. Thus, this region may be central in transforming tactile
332 information into an actionable spatial target. Third, coding of the movement goal was present
333 in a large network, consistent with regions shown to be involved in motor responses to visual
334 targets, suggesting similar coding of movements to tactile and visual targets.

335

336 ### Anterior PPC encodes touch in an anatomical reference frame

337 We identified regions that use an anatomical code for tactile location by testing which regions
338 could decode the foot on which the tactile stimulus was received, regardless of crossed or
339 uncrossed foot posture. Decoding was above chance in the SPL, a region in the anterior PPC,
340 as well as in a frontoparietal network of regions known to be involved in touch processing.
341 Previous work has demonstrated that anterior PPC contains regions that show selective
342 responses to tactile stimulation to different body parts[6,7,32,65]. In particular, a human fMRI
343 study identified a roughly homuncular tactile map in the SPL and anterior IPS that also
344 overlapped with retinotopic visual maps[7,65]. Tactile leg and toe regions in this map lay
345 medially, in close agreement with the SPL cluster for anatomical foot location found in the
346 present study (Fig. 8: yellow sphere number 1). Here, we report that this region uses an
347 anatomical code for tactile stimuli, that is, location is coded regardless of the current position
348 of the limb in external space. This anatomical stimulus coding in anterior PPC may not be
349 limited to tactile sensation. Human fMRI studies have identified coding of visual stimuli
350 relative to the position of the body in anterior PPC[25,26,29] (Fig 8: cyan spheres), suggesting that
351 anterior PPC may encode multisensory stimuli in relation to the body's layout or to the skin.
352 This finding extends the suggestion that rostral PPC "projects" the environment onto the body
353 and estimates the current state of the environment by transforming information to match
354 with the own body[32,66].

355

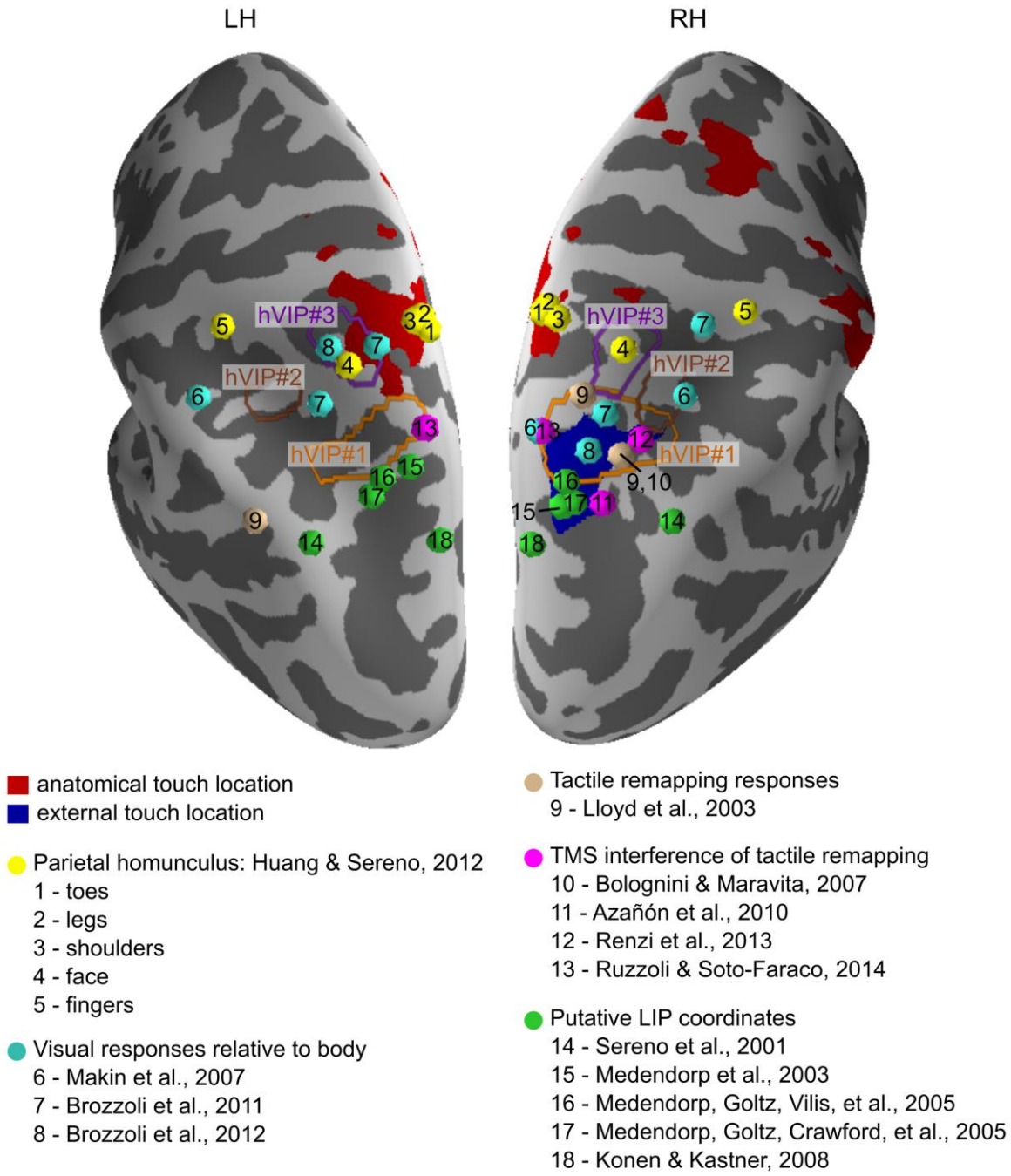

Fig. 8 Comparison of anatomical and external-spatial coding of tactile stimuli to coordinates from previous studies. Anatomical coding of touch location is overlayed in red and external-spatial coding of touch location is overlayed in blue. Outlines of the hVIP complex[32] are shown with hVIP#1 outlined in orange, hVIP#2 outlined in brown and hVIP#3 outlined in purple. Coordinates of the locations of body parts identified as a parietal homunculus[7] are shown in yellow. Coordinates of visual responses relative to the position of the body are shown in cyan. Coordinates of responses related to tactile remapping are shown in light brown. Locations of coordinates that were found to interfere with tactile remapping when stimulated using TMS are shown in pink. Locations of putative LIP coordinates are shown in green.

We decoded anatomical tactile stimulus location bilaterally in the medial bank of bilateral S1, adjacent to the SPL. This is consistent with the role of this region as the part of the somatosensory homunculus that responds to contralateral foot stimulation[1,2,67]. Regions

370 beyond S1 also exhibited sensitivity to the anatomical location of tactile stimuli, including the
371 left insula and the right IPL/S2, M1/S1 and PMd. Previous studies have also reported that these
372 regions respond to tactile stimuli[68–70], but had not yet specified the reference frame used to
373 encode these stimuli. Viewed together, these previous and our present results identify a
374 network of brain regions that encode tactile sensory location in an anatomical reference
375 frame.

376

377 **Posterior PPC encodes touch in an external-spatial reference frame**

378 We identified a region in the mIPS that encoded tactile stimulus location in an external-spatial
379 reference frame. This coding implies that the location has been abstracted from the skin
380 surface: a given location is coded relative to where it is in space, no matter on which body part
381 or skin location it was originally received. This external-spatial reference frame may be gaze-,
382 head-, or trunk-centered. We did not target these different possibilities in our study, and
383 accordingly did not vary gaze, head, and body position but instead kept all three aligned in our
384 experimental setup.

385 Nevertheless, the activated mIPS region partially overlapped with a region previously reported
386 as a putative human homologue of the lateral intraparietal area (LIP), which has been
387 associated with eye-centered coding[21,47,71–73] (Fig 8: green spheres). LIP encodes both visual
388 and auditory targets in an eye-centered reference frame[74–76] and it was therefore proposed
389 that LIP generally encodes stimuli of all modalities in an eye-centered reference frame[19]. Our
390 results are consistent with this proposal. Whereas LIP is often considered to be specific to
391 saccade planning, it has also been suggested to provide a sensory priority map[77,78].
392 Furthermore, LIP neurons are active during reaching movements[77,79]. This finding fits with
393 reports putative human homologue of LIP responds to both saccades and reaches[21,62,80–82].
394 Thus, a contribution of LIP to our present pointing task is consistent with previous findings,
395 especially given that we observed partial overlap between mIPS voxels initially coding tactile
396 stimuli in an external-spatial reference frame and later responding to the movement goal.
397 Overall, LIP's role in our delay task may be to first maintain salient spatial target information
398 and later to transform it into a motor goal once participants receive the pro/anti task rule.

399 However, the mIPS region we identified in our study also partially overlapped with hVIP#1, a
400 region that we have proposed to be one of three human homologue regions of macaque VIP[32].
401 Previous findings suggest that hVIP#1 encodes sensory stimuli in an external-spatial reference
402 frame[83], which again fits well with our present results. In sum, mIPS appears to encode tactile
403 information projected into an external-spatial code that is independent of the skin and is likely
404 anchored to the eyes.

405 Further support for a role of the LIP/ hVIP#1 region identified here in external-spatial coding
406 of touch has come from several TMS studies. Figure 8 depicts the respective stimulation
407 locations; three sites fall within hVIP#1[13,14,84], and one site lies more posteriorly, close to the
408 coordinates of the putative human LIP[12]. TMS to these locations impaired participants in
409 making judgments that required transforming tactile stimuli into a location in space[12],
410 appeared to impede, or modulate, the integration of arm posture in the context of tactile-
411 spatial processing[13,14], and impaired the integration of auditory cues with tactile processing in
412 external-space[84]. Despite their locational variability, a common aspect of all these studies was
413 that TMS interfered with the external-spatial processing of touch, thus suggesting that

414 posterior PPC plays a role in remapping tactile stimuli from an anatomical to and external-
415 spatial reference frame.

416 Decoding touch in space was only possible in the right hemisphere in our study. This finding is
417 consistent with the proposal that right PPC may be specialized for spatial somatosensory
418 function, as somatosensory deficits related to spatial processing are more frequent following
419 lesions in the right PPC as compared to the left PPC[85,86]. However, it is inconsistent with the
420 widely held idea that each hemisphere of PPC represents mainly the contralateral side of
421 space, and findings that both putative human LIP and hVIP#1 are bilateral regions[21,32,47,71,73].
422 FMRI responses related to tactile remapping in PPC were stronger in the right hemisphere in
423 one study[87], but in the left hemisphere in another study[88]. TMS studies on tactile remapping
424 have often targeted only the right hemisphere, making it unclear whether their findings would
425 generalize to the left hemisphere[12,13,84], however one study that stimulated both the left and
426 right hemisphere found similar effects for both hemispheres[14]. In sum, the available evidence
427 across fMRI studies is currently inconclusive and the reasons for the present, unilateral
428 activation remains unclear.

429

430 ## The brain maintains multiple reference frames concurrently

431 The overall picture that emerges is that anterior and posterior PPC regions play opposite roles
432 in spatially coding tactile stimuli. Anterior regions relate the environment to the body and,
433 thus, code space anchored to individual body parts. In contrast, posterior regions relate the
434 body to the environment and code information in an external-spatial reference frame,
435 potentially anchored to the direction of gaze (see [66]). Thus, PPC concurrently encodes touch
436 in both anatomical and external-spatial reference frames. Our study is the first to explicitly
437 disentangle the brain regions that encode tactile location in body- and space-based reference
438 frames at high spatial resolution. However, behavioural[89–91], electrophysiological[10,11,92] and
439 magnetoencephalographic[9,52] studies have also demonstrated that tactile information is
440 encoded in multiple, concurrently active, reference frames.

441 We have recently suggested that tactile processing may not rely on external-spatial coding by
442 default. Note, however, that the present task explicitly required the use of the external-spatial
443 location of touch. Therefore, representation of tactile location already during the sensory trial
444 phase, in which movement was not yet specified, may have been induced by the general task
445 requirements.

446 Finally, we note that PPC also responds to changes in body posture[49–51,93], suggesting that PPC
447 probably encodes information about current body posture. We did not directly address the
448 coding of body posture – crossed vs. uncrossed feet – in the present study. This is because we
449 manipulated posture across runs, so that any differences between postures identified by
450 MVPA could be attributable to unknown differences between runs, rather than limb crossing
451 per se.

452

453 ## Goal-directed pointing recruits similar networks independent of target modality

454 Once both target and task rule had been defined and participants could plan the required
455 action, a large network spanning multiple regions in premotor cortex, primary sensorimotor
456 cortex, and PPC selectively represented spatial information about the movement goal. This

network closely corresponded to the frontoparietal network involved in visuomotor planning[82,94–99]. Although regions of both hemispheres contained movement planning information, a more extensive area of the left, than right, hemisphere could decode the movement goal, and decoding accuracy was also higher in the left hemisphere. This is likely because participants pointed with their right hand. Regions coding the movement goal location included SPOC, the putative human homologue of the parietal reach region, and PMd; these two regions are thought to be involved in calculating the movement path from effector to target location[61,81,100,101]. The movement planning network also spanned the M1 hand area, SMA and pre-SMA, which are known to code preparatory movement signals related to the effector and target, as well as object-related movement intentions[55,57,102–104]. Lastly, the movement planning network also encompassed an anterior IPS region that has been linked to the preparation of grasping and pointing movements[16,62,105–107]. Altogether, these results identify a broad network of regions that encode the tactually-defined movement goal location and suggest that movement planning is very similar across sensory modalities of the target stimuli.

Sensory representations are only maintained as long as necessary

We were unable to decode sensory location information in the part of the trial in which the task rule had been specified and participants were, thus, able to plan the pointing movement. Classifiers trained to decode sensory location during the touch localization interval did not generalize to the movement planning interval, nor was decoding successful when we attempted to decode sensory location by both training and testing classifiers on responses during the movement planning interval. These findings suggest that sensory representations were only maintained for as long as necessary. Compatibly, previous fMRI work investigating visuomotor control has also demonstrated that sensory codes are only maintained as long as they are relevant in most regions[45,46], and recordings from PRR neurons in macaques have shown only brief, transient encoding of the visual target location when the movement cue is already known[40]. In the present study, brain regions that first encoded sensory information overlapped with those that later encoded movement planning (Fig. 7). This finding suggests that a dynamic sensorimotor transformation occurred in these regions once information to plan the pointing movement was available. Such overlap of target location and motor goal location across time has also been identified in the PMd and posterior IPS during visuomotor tasks[45], and equivalent dynamics have been identified in the coding of neurons in the macaque parietal reach region[40].

It has been proposed that a default motor plan could be made to one target during a delay period, and that this default plan would then later switch if the final cue requires using the non-prepared movement[108]. A default motor plan is unlikely to account for our present results, as the activation during the movement planning phase of trials was much more extended than that during the sensory phase, during which a default plan should have been evident if it existed. Furthermore, we found no evidence that coding was maintained across sensory target localization and motor planning intervals. Recordings from neurons in macaque LIP also support this conclusion: macaques delayed forming their decision until the final movement plan could be made, even when sensory decision information was already available[109]. Thus, altogether PPC appears to flexibly change its coding from sensory processing to motor preparation.

503 ## Posterior parietal cortex encodes the movement task rule.

504 We decoded the movement task rule (i.e., pro- vs. anti-pointing movement) from bilateral PPC
505 clusters in the SPL and SPOC. Several previous human fMRI studies that employed an anti-task
506 visuomotor paradigm did not observe differences in univariate activation evoked during
507 planning of pro- and anti-movements[41,45]. However, another study reported regional
508 differences for pro- and anti-pointing movements[39]. Yet another study was unable to identify
509 regions representing the task rule using a decoding approach[46], though that study used a
510 region of interest approach and may therefore have overlooked task rule encoding in areas
511 outside the inspected regions. In contrast to these human fMRI studies, responses of neurons
512 in monkey PRR were modulated by the pro/anti task rule[40], and PPC neurons encoded task
513 rule information independent of specific sensory cues[64]. In our study, the bilateral SPL and
514 SPOC regions that encoded the task rule almost completely overlapped with regions that
515 encoded the movement goal. The respective left SPL cluster additionally overlapped with the
516 SPL cluster that had previously encoded the anatomical tactile target location. These findings
517 suggest that PPC regions simultaneously encode multiple features at the population level[110].

518

519 ## Conclusion

520 Our study reveals the dynamic representation of spatial information during tactile
521 sensorimotor planning. Spatial codes in PPC were characterized by distinct multivariate
522 activation patterns that changed their selectivity from representing sensory information
523 during target localization, to representing the movement goal during motor planning. Tactile
524 sensory information was encoded in parallel in anatomical and external-spatial reference
525 frames. These different codes were evident in distinct PPC locations along an anterior to
526 posterior gradient, consistent with recent proposals that PPC contains poles that relate the
527 environment to the body (anterior) and vice versa (posterior). Once the movement task rule
528 was specified, tactile information was no longer detectable, and instead a frontoparietal
529 network encoded the location of the movement goal. Information about the tactile stimulus,
530 movement goal and the movement task rule converged in the left SPL, suggesting this region
531 may play a key role within the network that transforms tactile location into a movement plan.
532 Overall, the posterior parietal cortex integrates sensory information of the different sensory
533 modalities provided in different reference frames and flexibly combines this information to
534 plan movement towards both the environment and the own body.

535

536

Methods

Participants. The analyzed sample consisted of 16 students of the University of Hamburg (11 female), mean age 23.8 years (range: 19-30 years). Participants were right-handed according to questionnaire-guided self-report[111], had normal or corrected-to-normal vision, and reported to be free of any neurological disorders, movement restrictions, or tactile sensitivity problems. Participants provided written informed consent and received course credit or € 8/hour for their participation. Three further participants were excluded from analysis: one had performed >99% of all movements to the incorrect movement goal in the crossed, but not in the uncrossed foot posture, and MR slice positioning accidentally omitted part of SPL for the other two.

The experiment was approved by the ethics committee of the German Association of Psychology (Deutsche Gesellschaft für Psychologie, DGPs, TB 102011 and TB 102011_add_092014).

Behavioral Task. Participants planned and executed right hand movements toward tactile stimuli presented on the feet, while blood oxygenation level dependent (BOLD) signal changes in the brain were recorded using fMRI. A delayed movement task separated tactile localization, movement planning and movement execution into separate phases[21,61,62,81,82,112]. Fig. 1 illustrates the four phases of each trial: fixation (duration: 1 TR = 1880 ms), tactile localization on the foot (duration: 1-4 TR = 1880-7520 ms, in steps of 1 TR), movement planning of the right index finger (duration: 1-4 TR = 1880-7520 ms, in steps of 1 TR), and movement execution (duration: 1 TR = 1880 ms). The tactile stimulus occurred pseudo-randomly on the back of the left or right foot, either medially or laterally, approximately two centimeters below the heads of the metatarsal bones. Using two different locations on each foot encouraged participants to plan precise pointing movements rather than merely gesturing towards the left or right side. Critically, the tactile stimulus was not informative about the movement that would be required later in the trial: at the beginning of the movement planning delay, a visual cue indicated whether the pointing movement should be planned directly toward the tactile stimulus (pro-movement) or toward its mirrored location (anti-movement). It was only at this point in time that participants could derive the full movement plan. Finally, a visual cue prompted execution of the finger pointing movement.

In different experimental blocks, participants assumed either an uncrossed or crossed foot posture. The crossed posture allows anatomical and external locations of tactile stimuli to be dissociated as, for example, a stimulus on the anatomically right foot is then located in the left side of space.

The experiment comprised 3 within-subject factors. Foot Posture (levels: uncrossed vs. crossed) was maintained for 3 runs in a row, with the start posture alternated between sessions and counterbalanced across participants. We chose to minimize posture changes during the experiment to avoid fMRI and movement video recording artefacts due to changes in head and hand position. Stimulated Foot (left vs. right foot; collapsed across the medial and lateral stimulus locations on each foot) and Instructed Movement (pro-movement vs. anti-movement) varied from trial to trial. Trials were distributed into blocks of 33 trials each, with additional rest phases of 11 and 4 TR at the beginning and end of each run, respectively. We minimized dependencies between trials by balancing the trial sequence run-wise such that each condition was followed by every other condition equally often[113]. These order

restrictions required slightly different total trial numbers per experimental condition (48-51 trials) across the entire experiment. We minimized dependencies between the different trial phases within trials by choosing, from 1000 design matrices with randomized delays, the sequence that had the smallest correlations between the predictors in a General Linear Model (GLM) that contained the three factors of our experimental design. We used 4 different randomization protocols (sequence and timing) across the participant sample.

Experimental setup. Participants lay supine in the MR scanner with their head stabilized by foam cushions. The right hand was cushioned into a fixed position on the belly at the left-right body midline, with the index finger extended toward the feet. Experimental instructions were displayed on a monitor, projected onto a translucent screen in the scanner bore. Participants saw the projectors' image above their head through a mirror mounted on the head coil. Accordingly, participants directed their gaze upward and could not see their hands and feet. An infrared LED was taped to the index finger to record finger movements with a video camera placed in a window between the MR and control rooms. To improve the visibility of the IR LED, cardboard was placed above the right wrist, just below the chest, to shield light emitted from the projector at the end of the scanner bore.

After three blocks of a recording session, the experimenter passively moved the participant's legs into the required uncrossed or crossed position. Participants chose before the beginning of the experiment which leg should be on top, based on comfort. The crossed posture was fixed using cushions. If necessary for comfort, the top leg was slightly elevated using additional cushions placed below the knee. Direct skin contact of legs and feet in the crossed posture was prevented using clothing and towels to avoid the generation of conductor loops.

Experimental protocols were synchronized with volume acquisition (TR = 1880 ms) and controlled via the software Presentation, version 17.0 (Neurobehavioral Systems, Albany, USA). The fMRI experiment was conducted in two sessions, each about 2 hours long including 1 hour of preparation and 1 hour of scanning. The two scanning sessions were scheduled between several hours and 3 weeks apart. All experimental conditions were spread equally across the two scanning sessions. Participants completed a total of 12 experimental runs of 8 minutes duration each. Participants rested between runs and continued with the next run whenever they were ready.

Task practice. Participants practiced the task in a regular lab a few days before the first scanning session. Participants lay supine in a reclinable chair, and the visual display was mounted above the head, to mimic the fMRI environment. During practice, we monitored eye movements electrically with an EOG setup. Participants practiced the task until they executed the pointing movement at the correct time during the trial, aimed at the correct location, and kept the hand still at all other times. Furthermore, participants fixated a centrally presented cross throughout the task and practiced keeping the body and the head still during pointing movements.

Tactile stimulation. For tactile foot stimulation, we applied 2 ms electrical pulses through custom-built electrodes attached to a constant current electrical stimulator (DS7A; Digitimer, Hertfordshire, United Kingdom). A manual switch (DSM367; Digitimer, Hertfordshire, United

Kingdom) ensured that only a single location could be electrically stimulated at any time. One LED was placed near each of the four switch positions. At any time, one LED was illuminated and indicated the currently required electrode, and an experimenter continually adjusted the switch accordingly.

Before the experiment, the experimenter adjusted the current intensity separately for each electrode. A first electrode was adjusted, starting at 30 mV and increasing in steps of 30 mV until the participant reliably detected stimulation. Afterwards, the experimenter adjusted the threshold across the four stimulus locations until the participant indicated that all four stimuli felt equally strong and could all clearly be detected. We asked participants between runs whether tactile stimuli were still clearly detectable and increased stimulus intensity if it felt weak, or decreased it if stimulation became uncomfortable over time. On average, the selected stimulation intensity was 268.33 mV (range: 60-600).

Eye tracking. Participants had to maintain fixation throughout the experiment to avoid confounding effects of saccade planning and execution. We monitored the right eye's fixation with an fMRI-compatible eye tracker (Eye Link; SR Research, Ottawa, Canada) operated at a frame rate of 250 Hz. Eye tracker calibration used a 9-point fixation procedure before each scanning session. We identified saccades offline as a 2 s.d. deviation from the trial's mean eye position that also exceeded 20 pixels (0.5° of visual angle) on the presentation monitor. We excluded trials containing saccades from the fMRI data analysis.

Hand movement tracking. We recorded finger movements through a window that directly faced the scanner bore from the control room, using an IR-sensitive video camera operated at a frame rate of 40 Hz. In addition to the IR LED on the participant's finger, two color LEDs placed directly in front of the camera signaled the location of the tactile stimulus (left vs. right foot) and the instructed movement (pro vs. anti-movement) on each trial, allowing us to align video with fMRI data offline. We extracted finger position and movement direction (left vs. right, as seen from the participant's viewpoint) from the video with a custom-made, semi-automated procedure that was based on a combination of cluster detection methods, gradual averaging, and subtraction of images and automatically detected the changes of finger position across frames.

Data selection. We acquired 6303 trials after excluding one run of one participant due to a recording error. We excluded trials if the pointing movement was executed toward the wrong goal location (4.7%), when saccades occurred (10.2%) or when a combination of any of these occurred (0.5%). Hand movement data was unavailable or of low quality such that hand movements could not be determined in 34.0% of trials, for instance due to adverse lighting conditions or elevated foot position. Eye movement data was unavailable or low quality in 20.8% of trials, usually due to obstruction by the head coil. 7.6% of trials had unavailable or low-quality data for both hand and eye movements. Given the comparably low number of errors in trials for which all data was available, we did not exclude trials due to missing hand and eye data. The final analysis was based on 5396 trials, that is, 85.6% of all recorded trials. The number of trials included in the final analysis was similar across conditions, with an

average of 42.2 trials per condition per participant (range across conditions: 41.1 – 43.1 trials per condition per participant).

FMRI acquisition. We obtained fMRI data with a 3-tesla MR scanner (Siemens, Erlangen) and 32-channel head coil, using an echo planar imaging (EPI) T2*-sensitive sequence that acquired 32 axial slices in descending order (in-plane voxel size: 3 x 3 mm; slice thickness: 3 mm; slice gap: 0.51 mm; TR: 1880 ms; TE: 30 ms; flip angle: 70°; FOV: 216 x 216 mm).

Structural MRI acquisition. We obtained a high resolution (1 x 1 x 1 mm) structural MRI image of each participant using a T1* sensitive MPRAGE sequence with 240 slices, for use in coregistration and normalization of functional data.

Preprocessing of imaging data. We preprocessed and analyzed fMRI data with the software Statistical Parametric Mapping (SPM12, Statistical Parametric Mapping; http://www.fil.ion.ucl.ac.uk/spm/), integrated into MATLAB R2015a (The MathWorks, Natick, USA). We discarded the first four volumes of each run to allow for spin saturation. We corrected fMRI data for susceptibility artifacts and rigid body motion by unwarping and alignment to the first image of the first session. Then, we corrected functional images for differences in acquisition time, and co-registered the individual T1 image to the mean functional image generated during realignment.

Multi-voxel pattern classification analysis. We used a multi-voxel pattern analysis (MVPA) approach to determine whether multivariate patterns of brain activation allow classifying different types of spatial codes used during tactile processing and movement planning. This approach involved determining which brain regions differentiate pairs of characteristics, such as left vs. right foot stimulation or left vs. right-side movement goal. Fig. 2, Fig. S1 and Fig. S2 illustrate the pairwise comparisons we conducted to decode tactile location (6 classifiers), movement goal location (1 classifier) and task rule (1 classifier).

We constructed participant-level GLMs that were optimized for subsequent classification. Spatial interpolations inherent in normalization and smoothing might degrade meaningful activation patterns[114]. Therefore, we calculated GLMs in non-normalized, participant space and without smoothing. We accounted for baseline drifts within runs by applying a high-pass filter (128 s), and for serial dependency within runs by using an autoregressive model. GLMs included 23 predictors that modeled experimentally induced variance of the measured BOLD signal in each voxel with delta functions marking the onsets of the particular delay, convolved, in turn, with the canonical hemodynamic response function. There were 2 baseline predictors, one for each foot posture (uncrossed, crossed) that modeled fixation delays at the beginning of each trial, as well as during the rest periods at the beginning and end of each run. Four predictors modeled the touch localization delay (uncrossed, crossed foot posture x stimulation of left, right foot). Eight predictors modeled the planning and movement execution delays (uncrossed, crossed foot posture x stimulation of left, right foot x pro-, anti-movement). Finally, all trial phases that contained behavioral errors were assigned to a common predictor. Recall, that foot posture was either uncrossed or crossed in a given run.

712 Therefore, any given run contained only 12 (1 baseline, 2 tactile locations, 4 planning, 4
713 execution, 1 error) of the 23 experiment-wide predictors.

714 We performed MVPA with The Decoding Toolbox[114], using run-wise β-images for the different
715 trial phases and experimental conditions estimated by the GLM that reflected the voxel-wise
716 amplitude of the hemodynamic response function. We used an L2-norm support vector
717 machine (SVM) as classifier in the implementation of LIBSVM[115], with a fixed cost of c = 1. For
718 whole-brain unbiased voxel selection, we applied a spherical searchlight with a radius of 4
719 voxels[54]. On each classification fold, the classifier was trained with input patterns from run-
720 wise β-images to differentiate between two classes, such as movement goal left vs. movement
721 goal right. Note that the two decoded classes were always present on both uncrossed and
722 crossed runs, thus balancing any overall response differences between different postures.
723 Classifier performance was validated with a leave-one-out cross validation design that
724 predicted each of the 12 runs after training based on the respective 11 other runs. We report
725 the mean decoding accuracy across all classification iterations, depicted at the center voxel of
726 a given searchlight region, as the measure of the overall generalization performance of the
727 classifier of that searchlight region. We repeated this procedure for all recorded voxels,
728 resulting in a whole-brain map of averaged decoding accuracy for the two tested conditions
729 across all test runs. For group-level statistical analysis, we normalized participant-level
730 accuracy maps to MNI space based on the transformation parameters obtained during
731 segmentation of the T1 image, and applied 6 mm Gaussian kernel smoothing. Across
732 participants and for each classifier, we tested which brain voxels contained accuracy values
733 that differed significantly from chance-level (50%) using a one-sample t-test[116,117]. Significance
734 was determined using whole-brain cluster-based permutation tests using an initial threshold
735 of $p<.001$ and a secondary family-wise error (FWE) correction rate of $p<.05$[118]. Voxels that
736 survive this correction for multiple comparisons indicate locations where the decoding
737 accuracy of the classifier is significantly better than chance for the differentiation between the
738 two tested conditions. Put differently, multivariate patterns surrounding the identified voxels
739 contain information about the differentiation between the two classes of interest, which is
740 interpreted as their feature representation[54,60,119–122]. Visualizations of significantly higher
741 than chance classification accuracy are based on mapping of activations identified in the 3D
742 brain volume onto an inflated atlas of the cortical surface (Conte-69 atlas)[123] using the
743 Computerized Anatomical Reconstruction and Editing Toolkit (Caret)[124].

744

745 **Regions of interest (ROI).** We visualized decoding accuracy by adapting an approach that
746 allows for inter-individual differences regarding anatomical and functional brain
747 organization[55,125]. First, we defined regions of interest (ROI) based on the group-level t-map
748 of significant above-chance decoding accuracy. For distinct local clusters, ROIs were created
749 as a sphere with 6mm radius centered on the voxel with the highest statistical significance for
750 decoding. For large clusters, we created several ROIs based on peaks within the cluster,
751 theoretical considerations, and delineation of regions suggested by previous studies. Second,
752 we extracted, for each individual participant, the decoding accuracy of all voxels contained in
753 each respective group ROI and identified the voxel with the highest decoding accuracy. We
754 created participant-specific ROIs around individual peak voxels, again sphere-shaped with a 6
755 mm radius. Some ROIs overlapped partially, and were therefore combined whenever they
756 spanned a similar anatomical location and showed similar means and variances of decoding
757 accuracy across subjects. Group mean, individual means and bootstrapped confidence

intervals of decoding accuracy were calculated with the Hmisc package[126] in R[127] and visualized using ggplot2[128]. We determined the structural brain regions that were associated with each ROI using the anatomy toolbox for SPM[129] and labeled them based on previous studies related to goal-directed reaching and pointing[97].

Data Availability

Relevant data will be made available for further analysis upon request.

Acknowledgements

We thank Selina Pradel and Lara Pleil for help with data acquisition. This work was funded by an Emmy Noether grant of the German Research Foundation (DFG) to T.H. (He 6368/1-1, 1-2, 1-3). WPM was supported by the Netherlands Organization for Scientific Research for this work (NWO-VICI: 453-11-001) and is currently supported by NWA-ORC- 1292.19.298.

Author contributions

J.K. contributed to study design, data acquisition, planning and execution of the analysis, figure creation, and writing of the manuscript. She was responsible for data acquisition. C.F. contributed to data analysis, figure creation, and writing of the manuscript. W.P.M. contributed to study design, planning of the analysis, and writing of the manuscript. T.H. contributed to study design, planning of the analysis and writing of the manuscript, and supervised the study.

Competing interests

The authors declare that they have no competing interests.

References

1. Penfield, W. & Boldrey, E. Somatic motor and sensory representation in the cerebral cortex of man as studied by electrical stimulation. *Brain* **60**, 389–443 (1937).
2. Roux, F., Djidjeli, I. & Durand, J. Functional architecture of the somatosensory homunculus detected by electrostimulation. *J. Physiol.* **596**, 941–956 (2018).
3. Heed, T., Buchholz, V. N., Engel, A. K. & Röder, B. Tactile remapping: from coordinate transformation to integration in sensorimotor processing. *Trends Cogn. Sci.* **19**, 251–258 (2015).
4. Tamè, L., Azañón, E. & Longo, M. R. A Conceptual Model of Tactile Processing across Body Features of Size, Shape, Side, and Spatial Location. *Front. Psychol.* **10**, 291 (2019).
5. Heed, T., Backhaus, J., Röder, B. & Badde, S. Disentangling the External Reference Frames Relevant to Tactile Localization. *PLOS ONE* **11**, e0158829 (2016).
6. Seelke, A. M. H. *et al.* Topographic Maps within Brodmann's Area 5 of Macaque Monkeys. *Cereb. Cortex* **22**, 1834–1850 (2012).
7. Huang, R.-S., Chen, C. -f., Tran, A. T., Holstein, K. L. & Sereno, M. I. Mapping multisensory parietal face and body areas in humans. *Proc. Natl. Acad. Sci.* **109**, 18114–18119 (2012).
8. Sereno, M. I. & Huang, R.-S. A human parietal face area contains aligned head-centered visual and tactile maps. *Nat. Neurosci.* **9**, 1337–1343 (2006).
9. Buchholz, V. N., Jensen, O. & Medendorp, W. P. Parietal oscillations code nonvisual reach targets relative to gaze and body. *J. Neurosci.* **33**, 3492–3499 (2013).
10. Schubert, J. T. W. *et al.* Oscillatory activity reflects differential use of spatial reference frames by sighted and blind individuals in tactile attention. *NeuroImage* **117**, 417–428 (2015).
11. Schubert, J. T. W. *et al.* Alpha-band oscillations reflect external spatial coding for tactile stimuli in sighted, but not in congenitally blind humans. *Sci. Rep.* **9**, 9215 (2019).
12. Azañón, E., Longo, M. R., Soto-Faraco, S. & Haggard, P. The posterior parietal cortex remaps touch into external space. *Curr. Biol.* **20**, 1304–1309 (2010).
13. Bolognini, N. & Maravita, A. Proprioceptive alignment of visual and somatosensory maps in the posterior parietal cortex. *Curr. Biol.* **17**, 1890–1895 (2007).
14. Ruzzoli, M. & Soto-Faraco, S. Alpha stimulation of the human parietal cortex attunes tactile perception to external space. *Curr. Biol.* **24**, 329–332 (2014).
15. Batista, A. P., Buneo, C. A., Snyder, L. H. & Andersen, R. A. Reach plans in eye-centered coordinates. *Science* **285**, 257–260 (1999).
16. Bernier, P.-M. & Grafton, S. T. Human posterior parietal cortex flexibly determines reference frames for reaching based on sensory context. *Neuron* **68**, 776–788 (2010).
17. Bhattacharyya, R., Musallam, S. & Andersen, R. A. Parietal Reach Region Encodes Reach Depth Using Retinal Disparity and Vergence Angle Signals. *J. Neurophysiol.* **102**, 805–816 (2009).
18. Bosco, A., Breveglieri, R., Hadjidimitrakis, K., Galletti, C. & Fattori, P. Reference frames for reaching when decoupling eye and target position in depth and direction. *Sci. Rep.* **6**, 21646 (2016).
19. Cohen, Y. E. & Andersen, R. A. A common reference frame for movement plans in the posterior parietal cortex. *Nat. Rev. Neurosci.* **3**, 553–562 (2002).
20. Marzocchi, N., Breveglieri, R., Galletti, C. & Fattori, P. Reaching activity in parietal area V6A of macaque: eye influence on arm activity or retinocentric coding of reaching movements? *Eur. J. Neurosci.* **27**, 775–789 (2008).
21. Medendorp, W. P., Goltz, H. C., Vilis, T. & Crawford, J. D. Gaze-Centered Updating of Visual Space in Human Parietal Cortex. *J. Neurosci.* **23**, 6209–6214 (2003).

22. Pesaran, B., Nelson, M. J. & Andersen, R. A. Dorsal Premotor Neurons Encode the Relative Position of the Hand, Eye, and Goal during Reach Planning. *Neuron* **51**, 125–134 (2006).

23. Bremner, L. R. & Andersen, R. A. Coding of the Reach Vector in Parietal Area 5d. *Neuron* **75**, 342–351 (2012).

24. Bremner, L. R. & Andersen, R. A. Temporal Analysis of Reference Frames in Parietal Cortex Area 5d during Reach Planning. *J. Neurosci.* **34**, 5273–5284 (2014).

25. Brozzoli, C., Gentile, G., Petkova, V. I. & Ehrsson, H. H. fMRI Adaptation Reveals a Cortical Mechanism for the Coding of Space Near the Hand. *J. Neurosci.* **31**, 9023–9031 (2011).

26. Brozzoli, C., Gentile, G. & Ehrsson, H. H. That's near my hand! Parietal and premotor coding of hand-centered space contributes to localization and self-attribution of the hand. *J. Neurosci.* **32**, 14573–14582 (2012).

27. Buneo, C. A., Jarvis, M. R., Batista, A. P. & Andersen, R. A. Direct visuomotor transformations for reaching. *Nature* **416**, 632–636 (2002).

28. Ferraina, S. *et al.* Reaching in Depth: Hand Position Dominates over Binocular Eye Position in the Rostral Superior Parietal Lobule. *J. Neurosci.* **29**, 11461–11470 (2009).

29. Makin, T. R., Holmes, N. P. & Zohary, E. Is That Near My Hand? Multisensory Representation of Peripersonal Space in Human Intraparietal Sulcus. *J. Neurosci.* **27**, 731–740 (2007).

30. Piserchia, V. *et al.* Mixed Body/Hand Reference Frame for Reaching in 3D Space in Macaque Parietal Area PEc. *Cereb. Cortex* **27**, 1976–1990 (2016).

31. Duhamel, J.-R., Colby, C. L. & Goldberg, M. E. Ventral intraparietal area of the macaque: congruent visual and somatic response properties. *J. Neurophysiol.* **79**, 126–136 (1998).

32. Foster, C., Sheng, W.-A., Heed, T. & Ben Hamed, S. The macaque ventral intraparietal area has expanded into three homologue human parietal areas. *Prog. Neurobiol.* **209**, 102185 (2022).

33. Graziano, M. S. A. & Cooke, D. F. Parieto-frontal interactions, personal space, and defensive behavior. *Neuropsychologia* **44**, 845–859 (2006).

34. Chen, X., DeAngelis, G. C. & Angelaki, D. E. Flexible egocentric and allocentric representations of heading signals in parietal cortex. *Proc. Natl. Acad. Sci.* **115**, E3305–E3312 (2018).

35. Leoné, F. T. M., Monaco, S., Henriques, D. Y. P., Toni, I. & Medendorp, W. P. Flexible Reference Frames for Grasp Planning in Human Parietofrontal Cortex. *eneuro* **2**, ENEURO.0008-15.2015 (2015).

36. Chafee, M. V. & Crowe, D. A. Thinking in spatial terms: decoupling spatial representation from sensorimotor control in monkey posterior parietal areas 7a and LIP. *Front. Integr. Neurosci.* **6**, (2013).

37. Freedman, D. J. & Ibos, G. An Integrative Framework for Sensory, Motor, and Cognitive Functions of the Posterior Parietal Cortex. *Neuron* **97**, 1219–1234 (2018).

38. Oristaglio, J., Schneider, D. M., Balan, P. F. & Gottlieb, J. Integration of Visuospatial and Effector Information during Symbolically Cued Limb Movements in Monkey Lateral Intraparietal Area. *J. Neurosci.* **26**, 8310–8319 (2006).

39. Connolly, J. D., Goodale, M. A., Desouza, J. F. X., Menon, R. S. & Vilis, T. A Comparison of Frontoparietal fMRI Activation During Anti-Saccades and Anti-Pointing. *J. Neurophysiol.* **84**, 1645–1655 (2000).

40. Gail, A. & Andersen, R. A. Neural Dynamics in Monkey Parietal Reach Region Reflect Context-Specific Sensorimotor Transformations. *J. Neurosci.* **26**, 9376–9384 (2006).

41. Gertz, H. & Fiehler, K. Human posterior parietal cortex encodes the movement goal in a pro-/anti-reach task. *J. Neurophysiol.* **114**, 170–183 (2015).

42. Hallett, P. E. Primary and secondary saccades to goals defined by instructions. *Vision Res.* **18**, 1279–1296 (1978).

43. Munoz, D. P. & Everling, S. Look away: the anti-saccade task and the voluntary control of eye movement. *Nat. Rev. Neurosci.* **5**, 218–228 (2004).

869 44. Zhang, M. & Barash, S. Neuronal switching of sensorimotor transformations for antisaccades. *Nature* **408**,
870 971–975 (2000).

871 45. Cappadocia, D. C., Monaco, S., Chen, Y., Blohm, G. & Crawford, J. D. Temporal Evolution of Target
872 Representation, Movement Direction Planning, and Reach Execution in Occipital–Parietal–Frontal Cortex:
873 An fMRI Study. *Cereb. Cortex* **27**, 5242–5260 (2017).

874 46. Gertz, H., Lingnau, A. & Fiehler, K. Decoding Movement Goals from the Fronto-Parietal Reach Network.
875 *Front. Hum. Neurosci.* **11**, 84 (2017).

876 47. Medendorp, W. P., Goltz, H. C. & Vilis, T. Remapping the Remembered Target Location for Anti-Saccades
877 in Human Posterior Parietal Cortex. *J. Neurophysiol.* **94**, 734–740 (2005).

878 48. Van Der Werf, J., Jensen, O., Fries, P. & Medendorp, W. P. Gamma-Band Activity in Human Posterior
879 Parietal Cortex Encodes the Motor Goal during Delayed Prosaccades and Antisaccades. *J. Neurosci.* **28**,
880 8397–8405 (2008).

881 49. Filimon, F., Nelson, J. D., Huang, R.-S. & Sereno, M. I. Multiple Parietal Reach Regions in Humans: Cortical
882 Representations for Visual and Proprioceptive Feedback during On-Line Reaching. *J. Neurosci.* **29**, 2961–
883 2971 (2009).

884 50. Parkinson, A., Condon, L. & Jackson, S. R. Parietal cortex coding of limb posture: In search of the body-
885 schema. *Neuropsychologia* **48**, 3228–3234 (2010).

886 51. Pellijeff, A., Bonilha, L., Morgan, P. S., McKenzie, K. & Jackson, S. R. Parietal updating of limb posture: An
887 event-related fMRI study. *Neuropsychologia* **44**, 2685–2690 (2006).

888 52. Buchholz, V. N., Jensen, O. & Medendorp, W. P. Multiple reference frames in cortical oscillatory activity
889 during tactile remapping for saccades. *J. Neurosci.* **31**, 16864–16871 (2011).

890 53. Macaluso, E., Frith, C. D. & Driver, J. Delay Activity and Sensory-Motor Translation During Planned Eye or
891 Hand Movements to Visual or Tactile Targets. *J. Neurophysiol.* **98**, 3081–3094 (2007).

892 54. Kriegeskorte, N., Goebel, R. & Bandettini, P. Information-based functional brain mapping. *Proc. Natl. Acad.*
893 *Sci. U. S. A.* **103**, 3863–3868 (2006).

894 55. Ariani, G., Wurm, M. F. & Lingnau, A. Decoding Internally and Externally Driven Movement Plans. *J.*
895 *Neurosci.* **35**, 14160–14171 (2015).

896 56. Barany, D. A., Della-Maggiore, V., Viswanathan, S., Cieslak, M. & Grafton, S. T. Feature Interactions Enable
897 Decoding of Sensorimotor Transformations for Goal-Directed Movement. *J. Neurosci.* **34**, 6860–6873
898 (2014).

899 57. Gallivan, J. P., McLean, D. A., Valyear, K. F., Pettypiece, C. E. & Culham, J. C. Decoding Action Intentions
900 from Preparatory Brain Activity in Human Parieto-Frontal Networks. *J. Neurosci.* **31**, 9599–9610 (2011).

901 58. Kim, J., Bülthoff, I., Kim, S.-P. & Bülthoff, H. H. Shared neural representations of tactile roughness
902 intensities by somatosensation and touch observation using an associative learning method. *Sci. Rep.* **9**,
903 77 (2019).

904 59. van Kemenade, B. M. *et al.* Tactile and visual motion direction processing in hMT+/V5. *NeuroImage* **84**,
905 420–427 (2014).

906 60. Kaplan, J. T., Man, K. & Greening, S. G. Multivariate cross-classification: applying machine learning
907 techniques to characterize abstraction in neural representations. *Front. Hum. Neurosci.* **9**, 151 (2015).

908 61. Beurze, S. M., de Lange, F. P., Toni, I. & Medendorp, W. P. Integration of Target and Effector Information
909 in the Human Brain During Reach Planning. *J. Neurophysiol.* **97**, 188–199 (2007).

910 62. Heed, T., Beurze, S. M., Toni, I., Röder, B. & Medendorp, W. P. Functional Rather than Effector-Specific
911 Organization of Human Posterior Parietal Cortex. *J Neurosci* **31**, 3066–3076 (2011).

912 63. Buneo, C. A. & Andersen, R. A. The posterior parietal cortex: Sensorimotor interface for the planning and
913 online control of visually guided movements. *Neuropsychologia* **44**, 2594–2606 (2006).

914 64. Stoet, G. & Snyder, L. H. Single Neurons in Posterior Parietal Cortex of Monkeys Encode Cognitive Set.
915 *Neuron* **42**, 1003–1012 (2004).

916 65. Sereno, M. I. & Huang, R.-S. Multisensory maps in parietal cortex. *Curr. Opin. Neurobiol.* **24**, 39–46 (2014).

917 66. Medendorp, W. P. & Heed, T. State estimation in posterior parietal cortex: Distinct poles of environmental
918 and bodily states. *Prog. Neurobiol.* **183**, 101691 (2019).

919 67. Dietrich, C. *et al.* Dermatomal Organization of SI Leg Representation in Humans: Revising the
920 Somatosensory Homunculus. *Cereb. Cortex* **27**, 4564–4569 (2017).

921 68. Avanzini, P. *et al.* Four-dimensional maps of the human somatosensory system. *Proc. Natl. Acad. Sci.* **113**,
922 E1936–E1943 (2016).

923 69. Pleger, B. & Villringer, A. The human somatosensory system: From perception to decision making. *Prog.*
924 *Neurobiol.* **103**, 76–97 (2013).

925 70. Ruben, J. *et al.* Somatotopic Organization of Human Secondary Somatosensory Cortex. *Cereb. Cortex* **11**,
926 463–473 (2001).

927 71. Konen, C. S. & Kastner, S. Representation of Eye Movements and Stimulus Motion in Topographically
928 Organized Areas of Human Posterior Parietal Cortex. *J. Neurosci.* **28**, 8361–8375 (2008).

929 72. Medendorp, W. P., Goltz, H. C., Crawford, J. D. & Vilis, T. Integration of Target and Effector Information in
930 Human Posterior Parietal Cortex for the Planning of Action. *J. Neurophysiol.* **93**, 954–962 (2005).

931 73. Sereno, M. I., Pitzalis, S. & Martinez, A. Mapping of Contralateral Space in Retinotopic Coordinates by a
932 Parietal Cortical Area in Humans. *Science* **294**, 1350–1354 (2001).

933 74. Brotchie, P. R., Andersen, R. A., Snyder, L. H. & Goodman, S. J. Head position signals used by parietal
934 neurons to encode locations of visual stimuli. *Nature* **375**, 232–235 (1995).

935 75. Snyder, L. H., Grieve, K. L., Brotchie, P. & Andersen, R. A. Separate body- and world-referenced
936 representations of visual space in parietal cortex. *Nature* **394**, 887–891 (1998).

937 76. Stricanne, B., Andersen, R. A. & Mazzoni, P. Eye-centered, head-centered, and intermediate coding of
938 remembered sound locations in area LIP. *J. Neurophysiol.* **76**, 2071–2076 (1996).

939 77. Bisley, J. W. & Goldberg, M. E. Attention, Intention, and Priority in the Parietal Lobe. *Annu. Rev. Neurosci.*
940 **33**, 1–21 (2010).

941 78. Gottlieb, J. P., Kusunoki, M. & Goldberg, M. E. The representation of visual salience in monkey parietal
942 cortex. *Nature* **391**, 481–484 (1998).

943 79. Quiroga, R. Q., Snyder, L. H., Batista, A. P., Cui, H. & Andersen, R. A. Movement Intention Is Better Predicted
944 than Attention in the Posterior Parietal Cortex. *J. Neurosci.* **26**, 3615–3620 (2006).

945 80. Chen, Y. *et al.* Allocentric versus Egocentric Representation of Remembered Reach Targets in Human
946 Cortex. *J. Neurosci.* **34**, 12515–12526 (2014).

947 81. Gallivan, J. P., McLean, D. A., Smith, F. W. & Culham, J. C. Decoding Effector-Dependent and Effector-
948 Independent Movement Intentions from Human Parieto-Frontal Brain Activity. *J. Neurosci.* **31**, 17149–
949 17168 (2011).

950 82. Heed, T., Leone, F. T. M., Toni, I. & Medendorp, W. P. Functional versus effector-specific organization of
951 the human posterior parietal cortex: revisited. *J. Neurophysiol.* **116**, 1885–1899 (2016).

952 83. Wall, M. B. & Smith, A. T. The Representation of Egomotion in the Human Brain. *Curr. Biol.* **18**, 191–194
953 (2008).

954 84. Renzi, C. *et al.* Spatial remapping in the audio-tactile ventriloquism effect: A TMS investigation on the role
955 of the ventral intraparietal area. *J. Cogn. Neurosci.* **25**, 790–801 (2013).

956 85. Sterzi, R. *et al.* Hemianopia, hemianaesthesia, and hemiplegia after right and left hemisphere damage. A
957 hemispheric difference. *J. Neurol. Neurosurg. Psychiatry* **56**, 308–310 (1993).

958 86. Vallar, G. Spatial Frames of Reference and Somatosensory Processing: A Neuropsychological Perspective.
959 *Philos. Trans. Biol. Sci.* **352**, 1401–1409 (1997).

960 87. Lloyd, D. M., Shore, D. I., Spence, C. & Calvert, G. A. Multisensory representation of limb position in human
961 premotor cortex. *Nat Neurosci* **6**, 17–18 (2003).

962 88. Crollen, V. *et al.* Visual Experience Shapes the Neural Networks Remapping Touch into External Space. *J.*
963 *Neurosci.* **37**, 10097–10103 (2017).

964 89. Badde, S., Heed, T. & Röder, B. Integration of anatomical and external response mappings explains crossing
965 effects in tactile localization: A probabilistic modeling approach. *Psychon. Bull. Rev.* **23**, 387–404 (2015).

966 90. Badde, S. & Heed, T. Towards explaining spatial touch perception: Weighted integration of multiple
967 location codes. *Cogn. Neuropsychol.* **33**, 1–22 (2016).

968 91. Mueller, S. & Fiehler, K. Mixed body- and gaze-centered coding of proprioceptive reach targets after
969 effector movement. *Neuropsychologia* **87**, 63–73 (2016).

970 92. Heed, T. & Röder, B. Common anatomical and external coding for hands and feet in tactile attention:
971 evidence from event-related potentials. *J. Cogn. Neurosci.* **22**, 184–202 (2010).

972 93. Wada, M. *et al.* Spatio-Temporal Updating in the Left Posterior Parietal Cortex. *PLoS ONE* **7**, e39800 (2012).

973 94. Blangero, A., Menz, M. M., McNamara, A. & Binkofski, F. Parietal modules for reaching. *Neuropsychologia*
974 **47**, 1500–1507 (2009).

975 95. Culham, J. C. & Valyear, K. F. Human parietal cortex in action. *Curr. Opin. Neurobiol.* **16**, 205–212 (2006).

976 96. Filimon, F. Human Cortical Control of Hand Movements: Parietofrontal Networks for Reaching, Grasping,
977 and Pointing. *The Neuroscientist* **16**, 388–407 (2010).

978 97. Gallivan, J. P. & Culham, J. C. Neural coding within human brain areas involved in actions. *Curr. Opin.*
979 *Neurobiol.* **33**, 141–149 (2015).

980 98. Medendorp, W. P., Buchholz, V. N., Van Der Werf, J. & Leoné, F. T. M. Parietofrontal circuits in goal-
981 oriented behaviour. *Eur. J. Neurosci.* **33**, 2017–2027 (2011).

982 99. Vesia, M. & Crawford, J. D. Specialization of reach function in human posterior parietal cortex. *Exp. Brain*
983 *Res.* **221**, 1–18 (2012).

984 100. Bernier, P.-M., Cieslak, M. & Grafton, S. T. Effector selection precedes reach planning in the dorsal
985 parietofrontal cortex. *J. Neurophysiol.* **108**, 57–68 (2012).

986 101. Fernandez-Ruiz, J., Goltz, H. C., DeSouza, J. F. X., Vilis, T. & Crawford, J. D. Human Parietal "Reach Region"
987 Primarily Encodes Intrinsic Visual Direction, Not Extrinsic Movement Direction, in a Visual–Motor
988 Dissociation Task. *Cereb. Cortex* **17**, 2283–2292 (2007).

989 102. Fabbri, S., Strnad, L., Caramazza, A. & Lingnau, A. Overlapping representations for grip type and reach
990 direction. *NeuroImage* **94**, 138–146 (2014).

991 103. Gallivan, J. P., McLean, D. A., Flanagan, J. R. & Culham, J. C. Where One Hand Meets the Other: Limb-
992 Specific and Action-Dependent Movement Plans Decoded from Preparatory Signals in Single Human
993 Frontoparietal Brain Areas. *J. Neurosci.* **33**, 1991–2008 (2013).

994 104. Gallivan, J. P., Johnsrude, I. S. & Flanagan, J. R. Planning Ahead: Object-Directed Sequential Actions
995 Decoded from Human Frontoparietal and Occipitotemporal Networks. *Cereb. Cortex* **26**, 708–730 (2015).

996 105. Astafiev, S. V. *et al.* Functional Organization of Human Intraparietal and Frontal Cortex for Attending,
997 Looking, and Pointing. *J. Neurosci.* **23**, 4689–4699 (2003).

998 106. Beurze, S. M., Toni, I., Pisella, L. & Medendorp, W. P. Reference Frames for Reach Planning in Human
999 Parietofrontal Cortex. *J. Neurophysiol.* **104**, 1736–1745 (2010).

1000 107. Konen, C. S., Mruczek, R. E. B., Montoya, J. L. & Kastner, S. Functional organization of human posterior
1001 parietal cortex: grasping- and reaching-related activations relative to topographically organized cortex. *J.*
1002 *Neurophysiol.* **109**, 2897–2908 (2013).

1003 108. Dekleva, B. M., Kording, K. P. & Miller, L. E. Single reach plans in dorsal premotor cortex during a two-target
1004 task. *Nat. Commun.* **9**, 3556 (2018).

1005 109. Shushruth, S., Zylberberg, A. & Shadlen, M. N. Sequential sampling from memory underlies action selection
1006 during abstract decision-making. *Curr. Biol.* **32**, 1949-1960.e5 (2022).

1007 110. Pouget, A., Dayan, P. & Zemel, R. Information processing with population codes. *Nat. Rev. Neurosci.* **1**,
1008 125–132 (2000).

1009 111. Oldfield, R. C. The assessment and analysis of handedness: The Edinburgh inventory. *Neuropsychologia* **9**,
1010 97–113 (1971).

1011 112. Leoné, F. T. M., Heed, T., Toni, I. & Medendorp, W. P. Understanding Effector Selectivity in Human Posterior
1012 Parietal Cortex by Combining Information Patterns and Activation Measures. *J. Neurosci.* **34**, 7102–7112
1013 (2014).

1014 113. Brooks, J. L. Counterbalancing for serial order carryover effects in experimental condition orders. *Psychol.*
1015 *Methods* **17**, 600–614 (2012).

1016 114. Hebart, M. N., Görgen, K. & Haynes, J.-D. The Decoding Toolbox (TDT): a versatile software package for
1017 multivariate analyses of functional imaging data. *Front. Neuroinformatics* **8**, 88 (2015).

1018 115. Chang, C.-C. & Lin, C.-J. LIBSVM: A Library for Support Vector Machines. *ACM Trans Intell Syst Technol* **2**,
1019 27:1-27:27 (2011).

1020 116. Haxby, J. V. *et al.* Distributed and Overlapping Representations of Faces and Objects in Ventral Temporal
1021 Cortex. *Science* **293**, 2425–2430 (2001).

1022 117. Haynes, J.-D. *et al.* Reading Hidden Intentions in the Human Brain. *Curr. Biol.* **17**, 323–328 (2007).

1023 118. Nichols, T. E. & Holmes, A. P. Nonparametric permutation tests for functional neuroimaging: A primer with
1024 examples. *Hum. Brain Mapp.* **15**, 1–25 (2002).

1025 119. Haxby, J. V., Connolly, A. C. & Guntupalli, J. S. Decoding Neural Representational Spaces Using Multivariate
1026 Pattern Analysis. *Annu. Rev. Neurosci.* **37**, 435–456 (2014).

1027 120. Haynes, J.-D. A Primer on Pattern-Based Approaches to fMRI: Principles, Pitfalls, and Perspectives. *Neuron*
1028 **87**, 257–270 (2015).

1029 121. Haynes, J.-D. & Rees, G. Decoding mental states from brain activity in humans. *Nat. Rev. Neurosci.* **7**, 523–
1030 534 (2006).

1031 122. Norman, K. A., Polyn, S. M., Detre, G. J. & Haxby, J. V. Beyond mind-reading: multi-voxel pattern analysis
1032 of fMRI data. *Trends Cogn. Sci.* **10**, 424–430 (2006).

1033 123. Van Essen, D. C. *et al.* Parcellations and Hemispheric Asymmetries of Human Cerebral Cortex Analyzed on
1034 Surface-Based Atlases. *Cereb. Cortex* **22**, 2241–2262 (2012).

1035 124. Van Essen, D. C. Cortical cartography and Caret software. *NeuroImage* **62**, 757–764 (2012).

1036 125. Oosterhof, N. N., Tipper, S. P. & Downing, P. E. Viewpoint (In)dependence of Action Representations: An
1037 MVPA Study. *J. Cogn. Neurosci.* **24**, 975–989 (2012).

1038 126. Harrell, F. E. Hmisc: A package of miscellaneous R functions. Programs available from https://CRAN.R-
1039 project.org/package=Hmisc. (2018).

1040 127. R Core Team. *R: A Language and Environment for Statistical Computing*. (R Foundation for Statistical
1041 Computing, 2014).

1042 128. Wickham, H. *Ggplot2: elegant graphics for data analysis*. (Springer, 2009).

1043 129. Eickhoff, S. B. *et al.* A new SPM toolbox for combining probabilistic cytoarchitectonic maps and functional
1044 imaging data. *NeuroImage* **25**, 1325–1335 (2005).

1045

1046

1047 ## Tables

1048 **Table 1.** Means and standard errors of group ROIs in MNI coordinates, grouped by
1049 classification analysis (anatomical touch location; external touch location; movement goal
1050 location, movement instruction). L, left hemisphere; R, right hemisphere. S1f, foot area of
1051 primary somatosensory cortex; ins, insula; SPL, superior parietal lobule; S1f, foot area of
1052 primary somatosensory cortex; M1/S1, primary motor cortex/ primary somatosensory cortex;
1053 IPL/S2, inferior parietal lobule/ secondary somatosensory cortex; PMd, dorsal premotor
1054 cortex; mIPS, medial intraparietal sulcus; M1h, hand area of primary motor cortex; S1h, hand
1055 area of primary somatosensory cortex; SMA, supplementary motor area; preSMA, pre-
1056 supplementary motor area; aIPS, anterior intraparietal sulcus; SPOC, superior parieto-occipital
1057 cortex; V5, middle temporal visual area.

Analysis	**Hemisphere-ROI**	**Mean**			**Standard Error**		
		x	**y**	**z**	**x**	**y**	**z**
Anatomical touch location	L-S1f	-5.6	-37.4	60.3	0.7	0.9	0.5
	L-ins	-35.8	-23.9	5.9	0.7	0.8	0.8
	L-SPL	-21.1	-43.3	64.2	0.4	0.3	0.7
	R-S1f	8.4	-42.2	63.1	0.5	0.4	0.4
	R-M1/S1	58.7	-16.9	28.4	0.7	0.9	0.6
	R-IPL/S2	50.6	-10.9	41.0	0.7	0.9	0.5
	R-PMd	23.9	-0.3	50.6	0.5	0.5	0.3
External touch location	R-mIPS	24.8	-59.2	51.3	0.5	0.5	0.6
Movement goal location	L-M1h	-31.7	-21.6	63.9	0.7	0.9	0.5
	L-S1h	-30.8	-29.3	50.8	0.6	0.9	0.7
	L-S1f	-3.6	-45.8	57.1	0.9	0.6	0.8
	L-PMd	-26.4	-7.8	60.5	0.6	0.8	0.8
	L-SMA	-7.9	-6.8	55.4	0.7	0.8	0.8
	L-preSMA	-10.1	-6.6	46.6	0.7	0.7	0.8
	L-aIPS	-34.9	-35.8	45.9	0.4	0.7	0.6
	L-SPL	-16.7	-53.3	59.0	0.4	0.3	0.4
	L-SPOC	-14.9	-79.9	37.2	0.5	0.4	0.6
	R-M1h	33.0	-21.8	64.4	0.6	1.1	0.5
	R-S1h	29.6	-30.4	51.3	0.7	0.8	0.6
	R-S1f	4.3	-45.4	56.2	0.8	0.6	0.7
	R-PMd	26.6	-7.9	62.0	0.6	0.9	0.7

	R-SMA	6.0	-6.6	55.6	0.5	0.8	0.7
	R-SPL	13.1	-55.3	56.5	0.4	0.4	0.5
	R-V5	39.0	-65.7	17.2	0.7	0.7	0.8
Movement instruction	L-SPL	-14.5	-58.2	58.3	0.2	0.5	0.4
	L-SPOC	-15.2	-77.5	46.6	0.8	0.5	0.7
	R-SPL	5.5	-59.4	55.1	0.7	0.5	0.5